Evaluation of Methodology to Make Radially Heterogeneous Blood Vessel Imitating Structures Using Polydimethylsiloxane

A Thesis

Presented to

The Faculty of the Department of Engineering Technology

University of Houston

In Partial Fulfillment

Of the Requirements for the Degree

Masters of Science

Engineering Technology

By

Glen J. De los Santos

December, 2014

Abstract

This work focuses on forming a synthetic blood vessel imitating structure using a biocompatible polymer to mimic the multi-layer mechanical properties of native arteries with radial heterogeneity. The main contribution is a novel experimental protocol that will enable future implementation of theoretical blood vessel mechanics. Most important to this application are that the concentric layers of the blood vessel wall have different mechanical properties. Polydimethylsiloxane (PDMS) is a mechanically tunable, biologically inert, silicone based polymer widely used in biomedical laboratories. The project began with mold development and design, continued to polymer preparation techniques, then sample production, and finished with sample testing, analysis, and data comparison. A production polymer protocol was tailored to ensure that the samples were consistent, multi layered, and semi-transparent. All samples were tested in a Biaxial Vascular Testing and Culturing Device (BVTCD). This device placed the samples under physiological temperature and hemodynamic conditions and stretched them axially and circumferentially. The circumferential tests were conducted for a range of transmural pressures (0-300 mmHg) at three different axial stretch lengths. Pictures of each sample were taken at every pressure increment and processed digitally using MATLAB to determine stretch changes. Force values were measured and recorded for each stretch increment during the axial tests. The results were analyzed and compared to natural tissue samples taken from a bovine carotid. The samples were mechanically characterized and was found to have higher stiffness than natural blood vessels. The protocol developed proved to be effective in producing radially heterogeneous layered PDMS samples with degassing methods that provided clarity throughout the structure.

Table of Contents

List of Figures

List of Tables

Chapter 1

Introduction

1.0

Cardiovascular disease is the leading cause of death in the United States (Roger et al. 2012) and bypass grafting is the most common type of open heart surgery. Synthetic blood vessels are an appealing alternative to autologous grafts due to their availability and economic advantages (Nerem and Seliktar 2001; Zhang et al. 2007). When designing a stent or graft for surgical procedures, the mechanical properties of the artery that will anastomose the graft must be taken into account (Xue and Greisler 2003; Yang et al. 2006). Mechanical mismatches have plagued synthetic grafts leading to graft failure and occlusion especially in small diameter grafts (Borschel et al. 2013; Chan-Park et al. 2009; Campbell and Campbell 2007).

There is abundant research on the topic of synthetic blood vessels resulting in forward progress (Yow et al. 2006; Campbell and Campbell 2007; Chan-Park et al. 2009; R. Chen and Hunt 2007; Sarkar et al. 2007; Nerem and Seliktar 2001), but a need still exists for the development of a synthetic vessel that is tailored to be patient specific and vessel specific mechanical behavior (Yow et al. 2006). For instance, the mechanical properties of a carotid artery and saphenous vein differ greatly under pressurization (J D Humphrey et al. 2009). Note that the saphenous vein is the vessel used in bypass grafts. The resulting pressure-diameter relationship can also be influenced by the axial stretch. Furthermore, the blood vessels of a juvenile are often more compliant than those of the elderly (Arribas, Hinek, and González 2006). The nonlinear mechanical properties of blood vessels are endowed by their composite structure which has a radially heterogeneous configuration with distinct layers. Figure 1 shows a diagram representation of what each layer in a synthetic radially heterogeneous vessel would potentially represent versus its natural vessel counterpart.

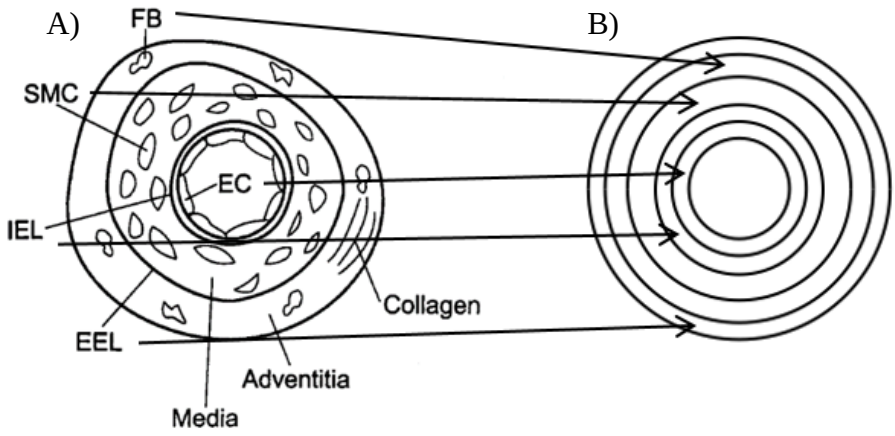

Figure 1: A) Diagram of a native blood vessel and its layers. FB is the fibroblast, SMC is smooth muscle cells, IEL is the internal elastic lamina, EEL is the external elastic lamina, and EC is endothelial cells (J D Humphrey et al. 2009). B) Diagram of a radially heterogeneous synthetic blood vessel with various layers that can potentially represent their natural vessel counterparts.

This project will contribute to the development of synthetic grafts and enable future research whereby the polymer can be functionalized and tailored to match certain mechanical properties of natural blood vessels (Cretich et al. 2008; Kurkuri et al. 2011). Although the future focus of this work is to improve the Coronary Artery Bypass Grafting (CABG) procedure, the technique is universal. The current project will focus specifically on the carotid artery due to its availability and relative straightness. This particular blood vessel is crucial to cerebral circulation and has been the target for a variety of vascular diseases including atherosclerosis (Arribas, Hinek, and González 2006; Wang et al. 2012).

Key methods for creating a radially heterogeneous blood vessel imitating structure start with the preparation of polydimethylsiloxane (PDMS). The basic mechanical properties are found in the Material Safety Data Sheet (MSDS) when mixed at the standard mixing ratio of 10:1 polymer base to curing agent. In order to reach the amount of axial and circumferential stress/stretch that a native blood vessels experiences, the mixing ratios will be altered. Each ratio has different mechanical properties (Khanafer et al. 2009). Another consideration is the material shape and dimensions that will be quantified during

biaxial testing. Basic uniaxial mechanical properties of PDMS were evaluated using a dog bone shaped samples that were tested on table top devices. The experimental environment for our mechanomimetic blood vessels is three-dimensional thus biaxial testing is required. The novel idea for this project is to test multi-layered tube shaped samples. In order to properly form the samples, a mold was needed. Through an iterative method, this mold was optimized, machined, and custom made to fit the sample dimensions. Mold design and testing were performed so that the best protocols can be used to create a finalized version. This end product was used to create viable samples for testing. Mechanical testing results were compared to natural tissue.

1.1 Project purpose

The main focus of this project was to develop a methodology to create radially heterogeneous blood vessel imitating structures using PDMS. When working with a man-made material, mechanical properties must be considered in the design including durability and longevity (Lillie and Gosline 2007). By focusing on mechanical properties, innovations in other vascular tissue engineering areas can stem from this research. Mechanical testing of natural arterial mechanical properties lead to an increased understanding of their biomechanical function (Gundiah, B Ratcliffe, and A Pruitt 2007; Lillie and Gosline 2007; Peterson, Jensen, and Parnell 1960). By finding a way to mimic these mechanical properties, an understanding of mechanical behavior in a biomimetic artery will be beneficial in the future treatment of damaged blood vessels and contribute to the development of preventative treatments for heart disease.

1.2 Biocompatible Polymers

Several common biological and synthetic polymers were considered for use in this research. Basic mechanical data for these synthetic polymers were found through research articles and compiled into a Criteria Matrix (Buckley et al. 2009; Gupta, Sinha, and Sinha 2010; Kim, Kim, and Jeong 2011; Subhash et al. 2010; Myung et al. 2007). as shown in Table 1. This is not an exhaustive list but highlights some of the most common materials used in biomedical laboratories. Each polymer described in Table 1 has advantages and disadvantages for use in bio-engineering, but the key component in our choice was a polymer with suitable mechanical properties which was both simple to use and safe.

Table 1: Criteria Matrix for Various Polymers.

Criteria Matrix										
Paper	Polymer	Linearity	Ultimate Engineering Stress	Ultimate Stress (kPa)	Engineering Strain at Ultimate	Engineering Stretch at Ultimate	Tunability	Biocompatibility	Surface Functionalization	Time of Synthesis
Q. Liu et al. (2010)	Agarose	Linear	50-140 kPa	50-140	12%-15%	1.12-1.15	Concentration	Yes	-	1-2 hours
D.J. Kelly et al. (2008)	Agarose	Non Linear	230 kPa	23	18%	1.18	Cooling Rate, Concentration	Yes	Yes	-
T.K. Kim et al. (2011)	PDMS	Non Linear	1.5 Mpa	1,500	120%	2.2	Concentration	Yes	-	-
Siddhi Gupta et al. (2010)	PVA	Non Linear	~ 90 Mpa	90,000	120%-350%	2.20-4.50	Concentration, # of Freeze Thaw Cycles	Yes	-	~14 days
Curtis W. Frank et al. (2007)	PEG	Non Linear	up to 6.45 Mpa	6,450	100%-215%	2-3.15	pH (UV-Light), MW of Monomer, Concentration	Yes	Yes	5 days

In order to thoroughly compare the various polymers, the engineering stress, stretch ratio, and mechanical tunability (often a concentration ratio) were graphed using MATLAB and Microsoft Excel. It was a requirement of the project to utilize a polymer that had a comparable stress value and stretch ratio to natural blood vessels which are shown on three dimensions in Figure 2. Mechanical tunability was used to influence the polymer's stress-stretch values. This was important because a multilayered synthetic artery needs layers with varied mechanical properties to imitate the residual circumferential stress found in functional blood vessels (Y. Chen and Eberth 2012). The concept of residual stress within arteries blood vessels were likely due to differential growth during development (Jay D. Humphrey and Delange 2004). In order to mimic these stresses, the ratio variation must start with a flexible, high stretch ratio on the inside and gradually increase stiffness to the outermost layer.

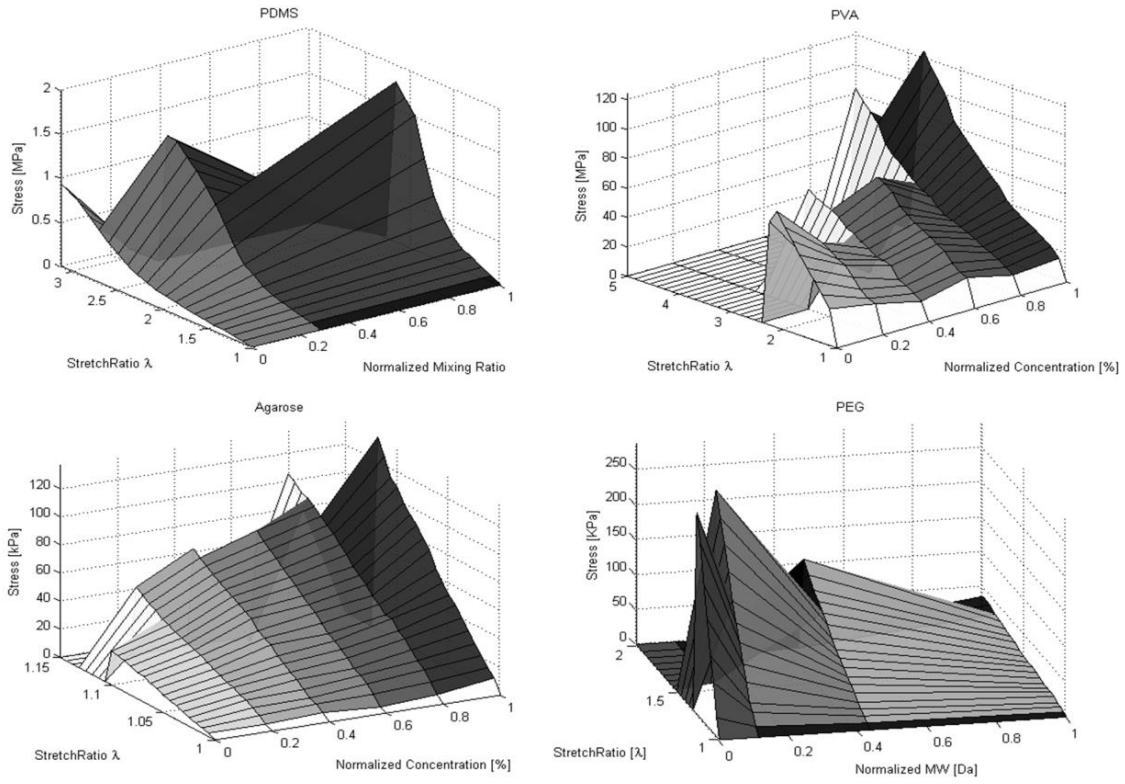

Figure 2: 3-Dimensional graph of PDMS, PVA, Agarose, and PEG polymers based on data collated from the literature.

Natural blood vessels have the capability to stretch 50-75% longer than its original length therefore, stretch ratio was a major concern. PDMS was chosen for the project because it was capable of stretching up to 50-75% of its original shape for all of its different mixture ratios and sustain these high stresses within human body conditions.

1.3 Polydimethylsiloxane

Polydymethylsiloxane or PDMS is a biocompatible polymer used for biomedical applications such as medical devices, artificial cornea applications, scaffolding for microfabrication processes, and to crosslink with other polymers (Quake and Scherer 2000; Jagur-grodzinski 2006; Enescu et al. 2008; Borenstein et al. 2007; Klenkler et al. 2005). PDMS also has a clear appearance, thermal stability, a low temperature performance, shear stability, and a good resistance to UV radiation (Kuo 1999). PDMS is often used for microfluidic systems and devices due to its ability to conform to various shapes in a master mold (Berdichevsky et al. 2004; Garra et al. 2002; Hum 2006; Leclerc, Sakai, and Fujii 2013). Though PDMS is hydrophobic and chemically inert there are methods for functionalization that will allow adhesion of live cells for various applications as well as creating porosity for high gas diffusion rates (Lopez et al. 2011; Linder et al. 2001; Lee et al. 2004; Cretich et al. 2008; Mata, Fleischman, and Roy 2005; Leclerc, Sakai, and Fujii 2013). This version of the silicone based elastomer is made using a Dow Corning Sylgard Elastomer 184 kit composed of a polymer base and curing agent. PDMS is formed by curing the liquid mixture; a process that can be accelerated with heat.

1.4 Objectives of this project

The overall objective of this report is to identify a method of producing a synthetic, radially heterogeneous blood vessel using PDMS and then compare the resulting mechanical characteristics with previously tested natural blood vessel samples. Although the purpose of this work is to generate nonlinear mechanical behavior from the radially heterogeneous vessel to be qualitatively similar to native tissue, future work will implement mechanical matching of the native and synthetic blood vessel properties. The synthetic arteries will be produced through a repetitive casting technique using molds that will shape PDMS into a three-dimensional solid. The vessels will be characterized using a Biaxial Vascular Testing and Culture Device (BVTCD) designed and built prior to this work. Here, samples undergo axial and circumferential stretch. Novel project tasks include the synthesis of a multilayered synthetic blood vessel using polydimethylsiloxane, developing protocols and methodology for production of samples, and mechanically testing these samples biaxially and comparing the results to natural animal blood vessel data tested under similar loading conditions.

Chapter 2

Materials and Methods

2.0

This section describes the materials and methods used in this research project to prepare and cure the biomimetic artery material. This includes the relevant equations, molding processes and the various mold designs and protocols encountered throughout the project. The discussion will follow with a description of tools and equipment used in preparation, dispensing, and curing the polymer. The discussion will continue with a brief description of the tools that were used to characterize the material samples.

2.1 Mechanical Preliminaries

The mechanical factors to consider in this experiment are stress and stretch. Stress is defined as "a force acting over an oriented area at any point of the body" (Jay D. Humphrey and Delange 2004). Laplace's circumferential stress (or hoop stress) equation is,

$$\sigma_\theta = \frac{Pa}{h}$$

Equation 1: Circumferential Stress equation

where P is the pressure, a is the luminal radius, and h is the wall thickness. The axial stress can be calculated by:

$$\sigma_z = \frac{f}{\pi h(2a + h)}$$

Equation 2: Axial Stress equation

where f is the axial force divided by the cross sectional area (J D Humphrey et al. 2009). Figure 3 illustrates the free body diagram of the forces imposed upon a cylindrical sample when placed under pressurization and axial distention.

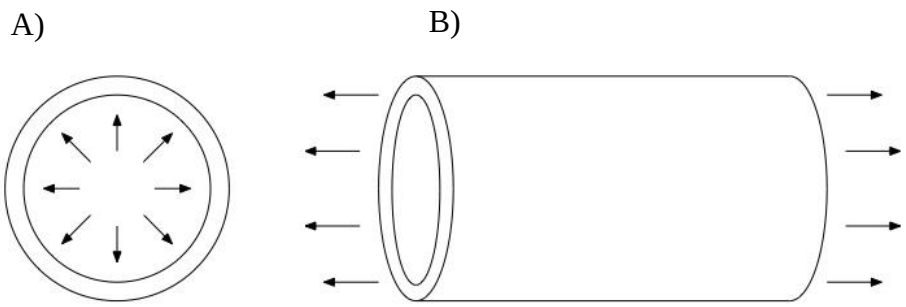

Figure 3: A free body diagram of the loads imposed on the sample under A) pressurization and B) axial distension.

The stretch was calculated using a ratio of the current dimension divided by the original dimension. The following equations describes the circumferential and axial stretch ratio calculations,

$$\lambda_\theta = \frac{b}{B}; \qquad \lambda_z = \frac{l}{L}$$

Equations 3-4: Circumferential and Axial Stretch Equations

where B, L, b, and l are the unloaded outer radius, unloaded length, loaded outer radius, and loaded length respectively. Measurements of the samples were performed using digital calipers and a force gauge.

The comparison of the samples to a natural blood vessels are generally assumed to be thin walled. However, the five layers that will form the samples are thick walled. This is determined by the rule of thumb for cylinder thickness, which is when the ratio of wall thickness, h, to the radius, r, is 1/20 or less the system is considered thin walled (Jay D. Humphrey and Delange 2004). A higher ratio will use the thick wall assumption. Each layer of the samples was only .05 mm thick, and the combination of five layers formed a thick walled vessel. Since the ratio of wall thickness to inner radius is 5/12, the samples are considered thick walled.

Thick walled cylinders have a more complex formula base because the stresses vary throughout the cylinder wall. The Lame equations (Jay D. Humphrey and Delange 2004) for radial and circumferential stress are:

$$\sigma_\theta = \frac{P_i a^2 - P_o b^2}{b^2 - a^2} - \frac{(P_i - P_o)a^2 b^2}{(b^2 - a^2)r^2}$$

Equation 5: Circumferential Stress equation

$$\sigma_r = \frac{P_i a^2 - P_o b^2}{b^2 - a^2} + \frac{(P_i - P_o)a^2 b^2}{(b^2 - a^2)r^2}$$

Equation 6: Radial Stress equation

where P_i is the inside pressure, P_o is the outside pressure, a is the inner radius, b is the outside radius, and r is any point between and b. The variables used for r are the inner wall diameter of each PDMS layer, which varied between 3 mm to 4.5 mm. Since internal pressure is the source of deformation in the samples, the outer pressure is assumed to be at zero. The internal pressures will range from 0-300 mmHg and plugged into Lame's equations. Each layer of the sample would also have a different stiffness since each is composed of a different ratio. Figure 4 shows the calculated stresses along the sample wall for each layer. The first layer experiences the most stress and those values become smaller progressively toward the outer layers. The radial stress in Figure 5 shows a similar trend as the circumferential stress but in the negative direction. Radial and circumferential directions show that they have equal but opposite behavior under pressure. These graphs will help predict what results are given from the testing.

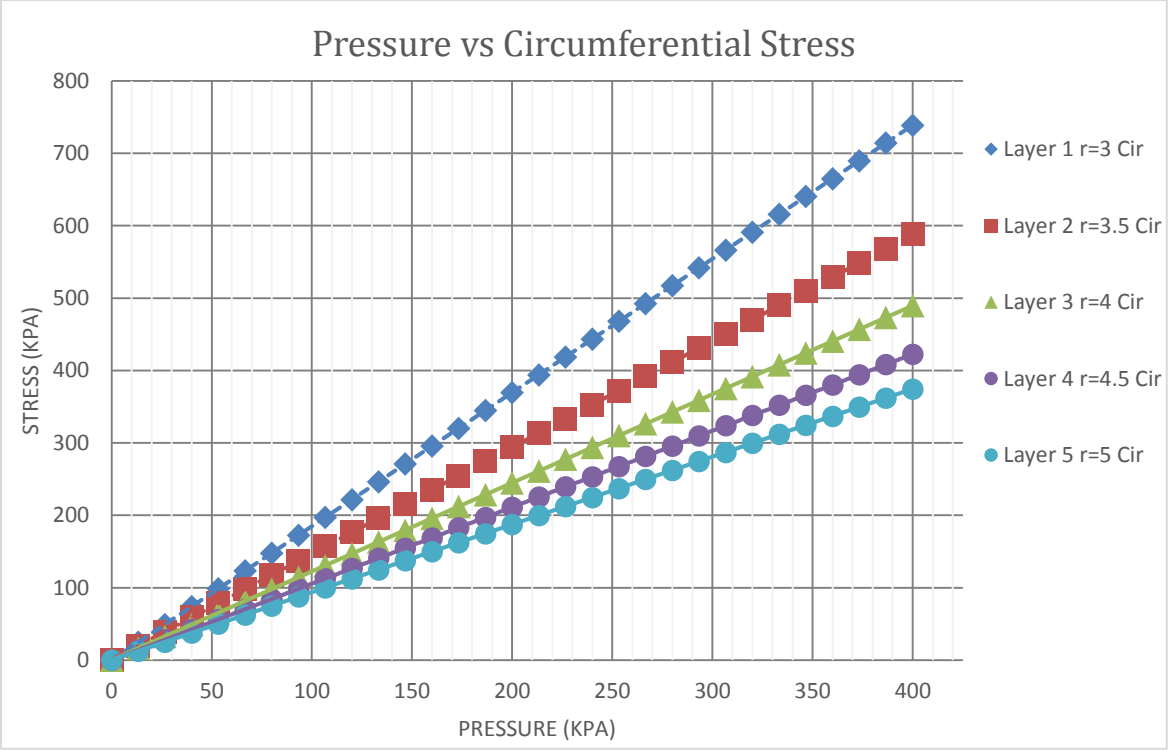

Figure 4: Pressure vs Circumferential Stress for each layer.

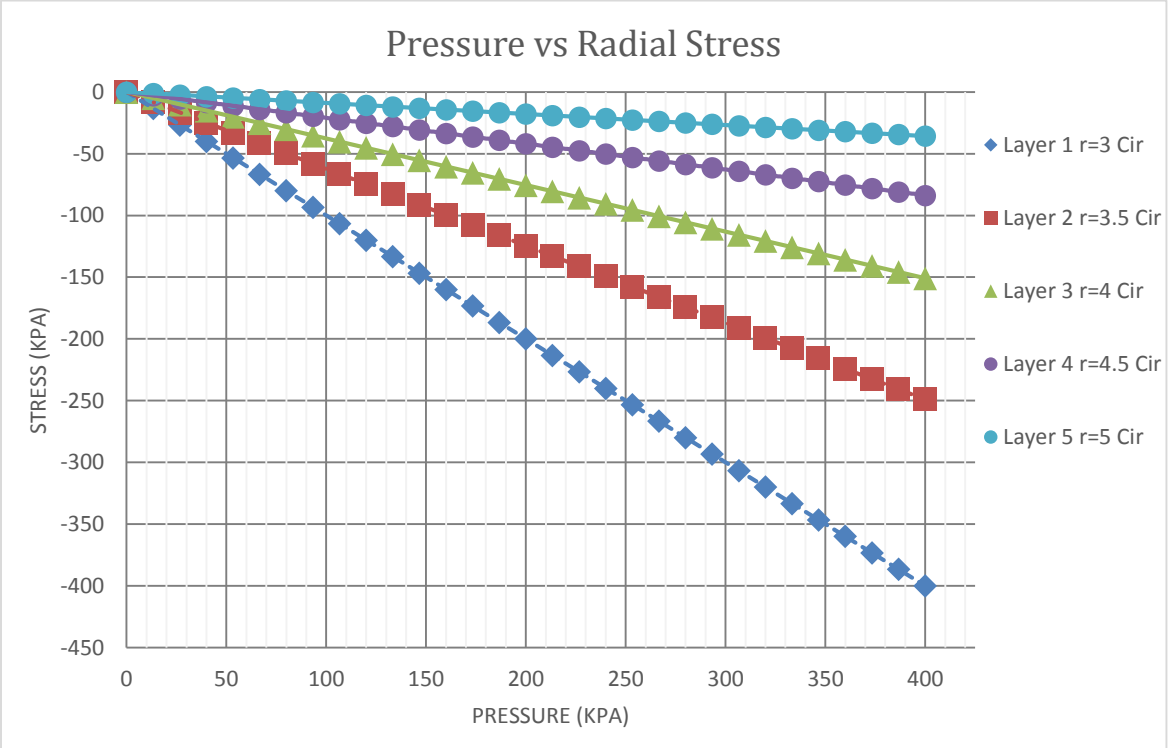

Figure 5: Pressure vs Radial Stress for each layer.

The axial stresses are constant throughout the cylinder wall. Equation 7 and Figure 6 show that internal pressure does not impact the stress axially throughout the cylinder wall. The stresses are constant and are the same for all 5 layers.

$$\sigma_z = \frac{P_i a^2 - P_o b^2}{b^2 - a^2}$$

Equation 7: Axial Stress equation

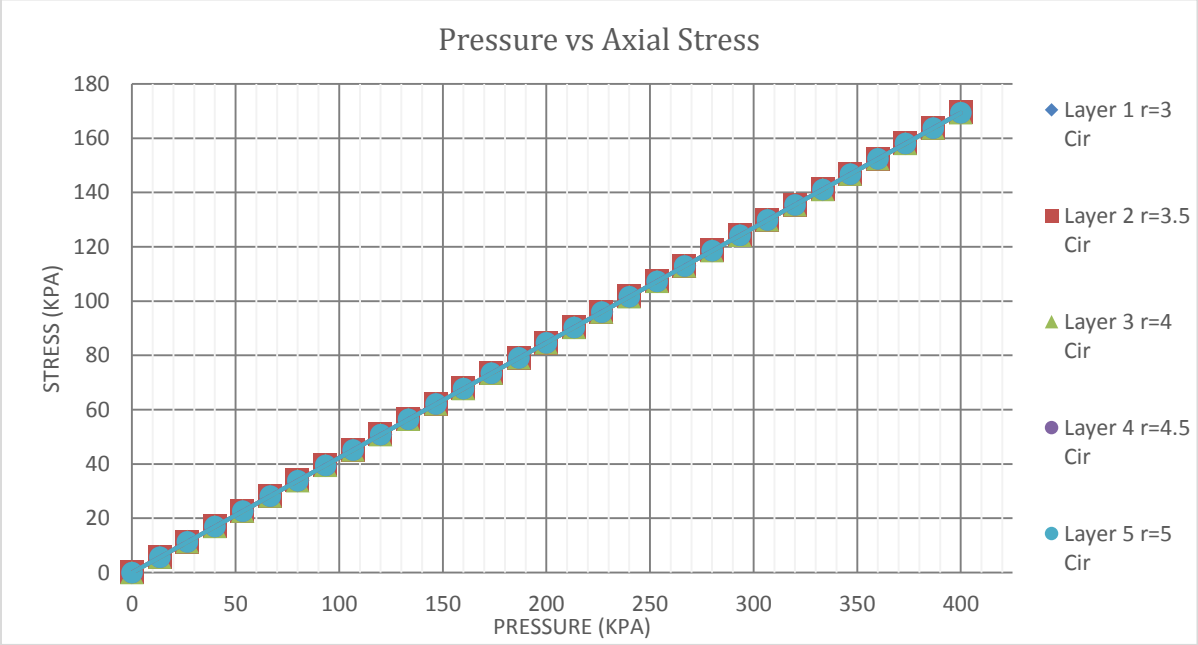

Figure 6: Pressure vs Axial Stress for each layer.

Further characterization of the sample such as stiffness would be determined through assumptions, which would simplify the data for processing. The layer stiffness and material stiffness are differentiated by the testing direction, where layer stiffness is found through circumferential stress and material stiffness is through axial stress.

2.2 Mechanical Testing

Research and testing of PDMS were performed using a Mark-10 uniaxial motorized test stand with 100 Lb force gauge. ISO 37 tests were performed using dog bone shaped in the Translational Biomechanics Laboratory (TBL) as shown in Figure 7. These tests were to confirm Khanafer et al's research and develop similar results.

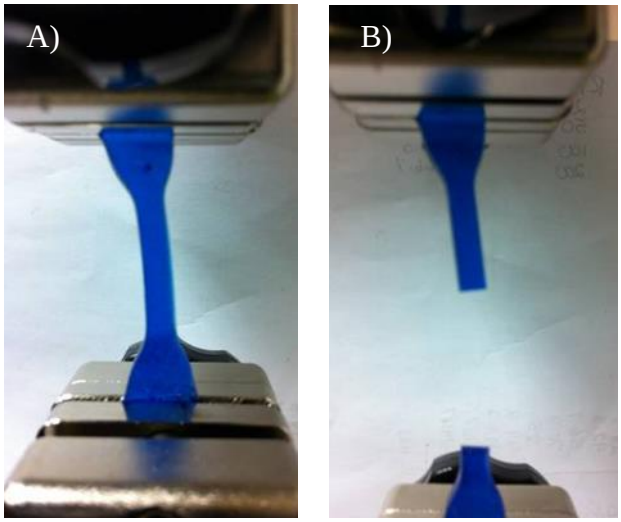

Figure 7: Tensile testing using a dog bone shaped PDMS sample in the TBL. A) Sample prior to stretching. B) Sample at failure.

The resulting curves, Figure 8 and Figure 9, demonstrate similar trends between the 50-100% strain values for the 7:1 and 10:1 ratios. The comparisons were made to confirm that a change in ratio does affect the stress/strain behavior in PDMS. The work performed in the TBL show that 10:1 ratio maintained a higher strain before failure. Hypothetically, a combination of these ratios layered within a cylindrical sample should express results that have moderate stretch ratios and sustain high pressure. When synthesized in layers, the distention of the various ratios within a common structure should express an elastic trend that fall within the data plots found in the TBL and Khanafer's research. The layer combinations and their elastic trend within a common structure are hypothetical and are tested within this project.

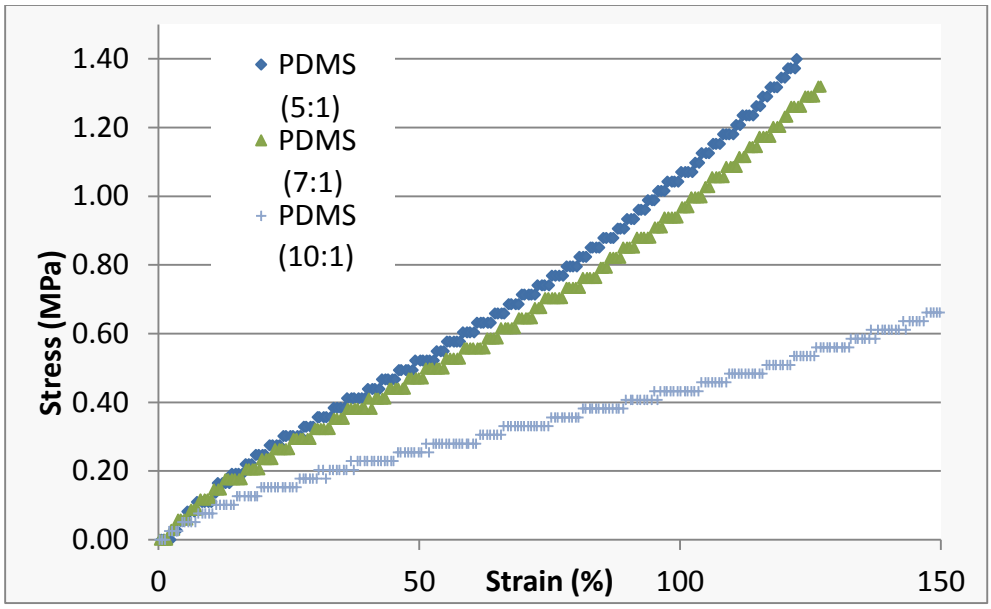

Figure 8: Engineering Stress vs Strain graph for 5:1, 7:1, 10:1 PDMS base polymer to curing agent ratios tested in the TBL.

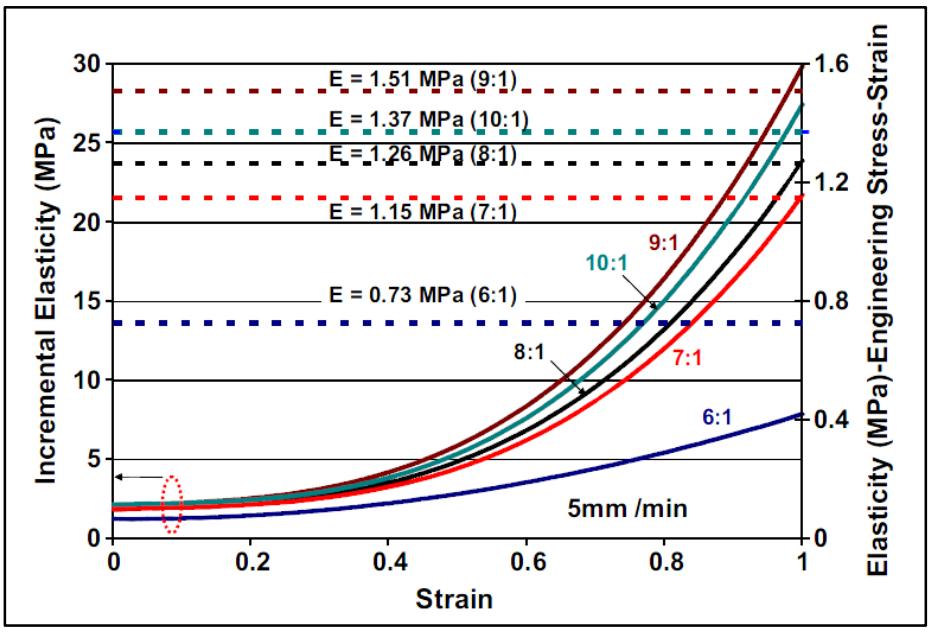

Figure 9: Engineering Stress (rightmost axis) vs Strain graph different PDMS ratios (Khanafer et al. 2009).

2.3 Biaxial Testing Device

The Biaxial Vascular Testing and Culturing Device (BVTCD) was designed and built by a Capstone Project in the Translational Biomechanics Laboratory (In progress). It was a student made project assembled with the intention to determine the mechanical properties of mammalian blood vessels while maintaining *in vivo* conditions and physiological geometry. The components of the BVTCD were controlled using LabVIEW.

During testing, physiological conditions were maintained using a continuous loop of saline solution provided by a peristaltic pump. Temperature of the two flow loops was controlled via a water heater with saline reservoirs submerged in the bath and looped through the system. Axial stretch was applied by varying the stepper motor positions and the force was recorded with an in-line force transducer. Circumferential stretch forces were applied by manipulating the transmural pressure values using a pressure controller that applies a pressure head on top of the transmural fluid within a compliance chamber. The circumferential stretch changes, via measurements of the outer diameter, were recorded by taking images during testing. Figure 7 shows an illustrated schematic of the BVTCD. The red line shows the continuous loop that flows through the sample vessel within the test chamber, the green represents the chamber fluid loop, the blue shows the airline input that maintains the fluid pressure, and the black line represent the electrical wiring. Figure 8 shows a photo of the device setup during sample testing. The testing chamber is identified on the image to indicate the testing area on the device.

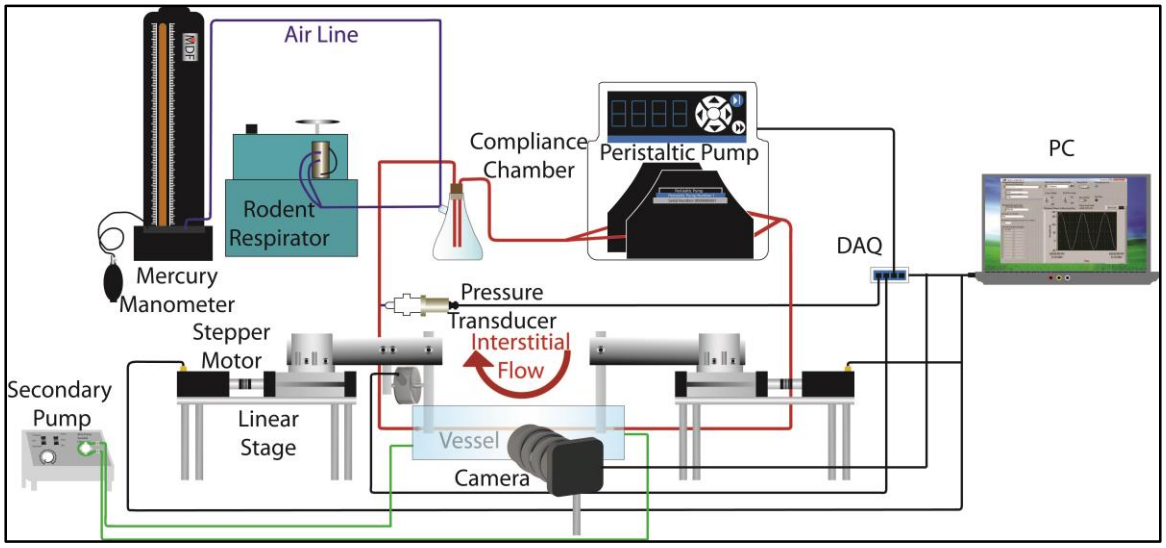

Figure 10: Biaxial Vascular Testing and Culturing Device Schematic.

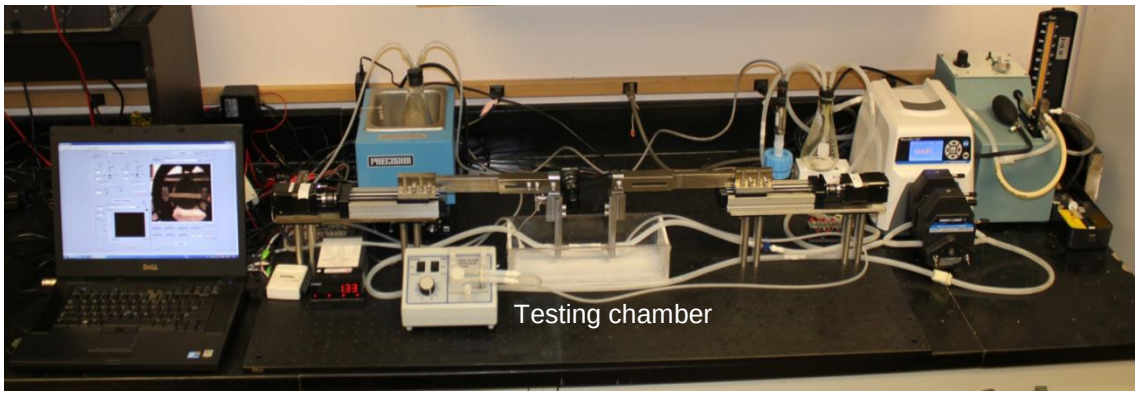

Figure 11: Biaxial Vascular Testing and Culturing Device. The testing chamber is identified to indicate the testing area on the device.

2.4 Optimization of the PDMS Preparation Protocol

2.4.1 Replication of Existing Protocols

These protocols were applied using information available from the Interdisciplinary Education Group, BioMEMS, and Dow Corning (Grigoriev et al. 2011; Kotz and Nagrath 2004). The information did not specify the type of ratio between the base and curing agent, so a weight ratio was used to maintain consistency. During initial testing, samples were cured at room

temperature overnight or for as long as 48 hours, until they were fully formed. Some were also placed on a hot plate and cured within manufacturer suggested times and temperatures:

35 minutes @ 100°C

20 minutes @ 125°C

10 minutes @ 150°C

Also, various methods were implemented to remove all air bubbles from the samples, but a minute amount always remained. Some were left undisturbed for one hour at room temperature to allow bubble floating to the surface. Other samples were agitated via tapping on the container to release the trapped air bubbles, which were then broken by blowing on the surface of the sample.

The next procedure replicated was taken from the Interdisciplinary Education Group. This procedure used a 10:1 weight ratio and sonication for air removal after mixing. Both a sonic bath and sonicator probe were used to speed up the removal of air bubbles from the mixture. The probe was placed in a water bath with the mixture in a test tube. A frequency of 35 MHz was used for both the sonic bath and sonicator probe for bubble dispersal. The mixture was cured on a hot plate for 20 minutes at 130°C.

The last procedure replicated was from BioMEMS. This process also called for a 10:1 weight ratio and incorporated a vacuum dessicator. A sample mixture was degassed for approximately 30 minutes. The dessicator was vented every 15 minutes to release the bubbles from the surface. The mixture was cured in a hot plate at 80°C for 3-6 hours.

2.4.2 Factors to Consider

2.4.2.1 Time

Multilayer samples required each layer to completely cure before synthesizing the next one. Therefore, time played a large factor in the PDMS preparation because the actions used in the

procedures such as pouring, weighing, mixing, transfer of containers, air bubble removal, and curing took over 5 hours for one layer.

2.4.2.2 Air

PDMS in its liquid state has the tendency to accumulate and trap air due to its high viscosity. Air bubbles form when the fluid is exposed to agitation where the liquid is forced into motion from rest. Forms of agitation originate mostly from the transfer of the mixture between containers. At least two transfers were performed during the protocol replications. The first one started in the mixing container. The stirring of the polymer base and curing agent introduced air initially into the mixture. The second transfer was to the mold or curing container where the PDMS would under-go air removal. Should a transfer to another container occur after the polymer has been de-aired, that mixture would need another air removal session.

2.4.2.3 Sample Removal

When fully cured polydimethylsiloxane retains the form of its container, and it also has a tendency to adhere to said container, making it difficult to remove. The removability varied between container materials and geometries. For example, PDMS was easier to remove from plastic boats than test tubes and other cylindrical containers. Flat vessels such as a microscope slide or weigh boats had easier removal than containers that have contact with PDMS on more than one surface. The difficulty of samples to remove was a concern due to the need for the sample to retain a smooth surface for testing.

2.4.3 PDMS Mold

Several mold concepts were evaluated to successfully synthesize a mechanomimetic artery into the correct shape and form. Factors that were also considered to evaluate potential molds

include: material type, design, and reusability. The hotplate deterred any considerations for polycarbonate or plastic material because they are temperature resistant and cannot provide adequate heat to cure PDMS in less than twenty four hours. Polycarbonate has a thermal conductivity of 0.22 W/(mK) compared to 205 W/(mK) of aluminum or 50.2 W/(mK) of steel (Young 1992; Serini 2002). Therefore, in order to utilize the hotplate a metal must be used. The type of metal needed to be machinable and have good heat conductivity. Aluminum was the chosen material because it not only met all of the fabrication requirements but also was readily available (Songmene et al. 1983).

The overall focus of the design was to make sure that the mold interior was capable of casting a smooth, cylindrical, symmetrical shape. Measures were also taken to ensure that all layers had the same quality. The first layer was considered the most important because it was the only section in the sample that had direct contact with the saline test fluid.

The final production protocol was affected by the mold design because it included a step in which air pockets are removed. The amount of time designated for degassing the mold was affected by its design version and orientation of the mold when curing on the hot plate. Each mold design was evaluated on its effectiveness in forming a radially heterogeneous structure and had major changes implemented on its next version. The mold design and preparation protocol both changed in conjunction with the design improvement to produce a repeatable method for synthesizing a quality PDMS sample. Four mold versions were designed and fabricated in the optimization of the PDMS production protocol as discussed here.

2.4.3.1 Production Mold

The Production Mold, also known as Mold Version 4, was the finalized iteration, used an elongated mold body and smoothed out interior surface. The smooth bores were achieved by using mechanical reamers. These tools created a smooth surface finish and also increased accuracy of a true cylinder within a given diameter. This was achieved by the removing material of about 0.1 mm from an under drilled hole. The material used was 6061 aluminum alloy. Guide shafts, with one side being a male end and the other female, were installed on the mating ends of the interior to help align the halves. The holding screw holes were also mounted on the same side, which made the tightening of both halves easier to handle and reduced spilling. Holes were drilled straight through for the center rod. Deep countersinks were placed on both ends of the holes and a new center rod was made with O-ring slots. Figure 12 shows a top view of the production mold identifying the deeper countersunk holes and also showing the new center rod with O-ring slots.

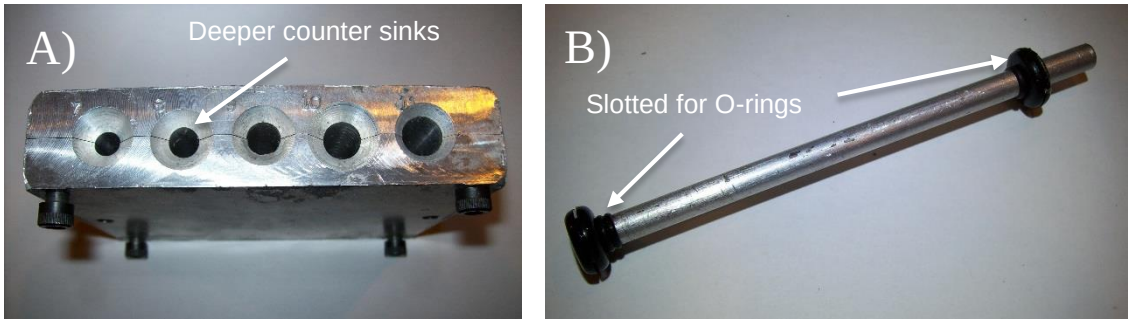

Figure 12: A) Top view of the Production Mold. B) New rod and end O-rings.

The custom washers from the previous mold versions were used for various applications, and varied for each bore size. Figure 13 shows a picture of the machined mold showcasing the improvements from previous designs. Alignment rods are identified in the figure, showing the accuracy of and reliability improvement in this design version.

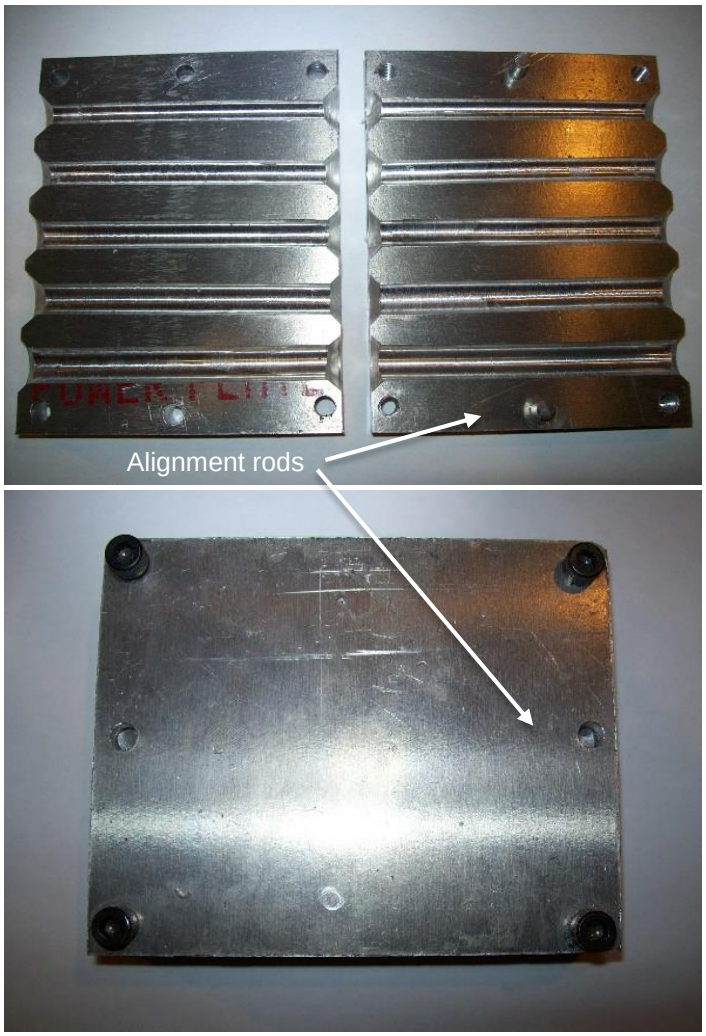

Figure 13: A) Production Mold view of interior. B) Assembled view with screws.

Figure 14 shows a computer generated image of the Production Mold showcasing a clearer depiction of the mold's design halves. This figure identifies the improvements at a more detailed level, including the location of the threaded holes that allowed the mold to efficiently be tightened on the same side.

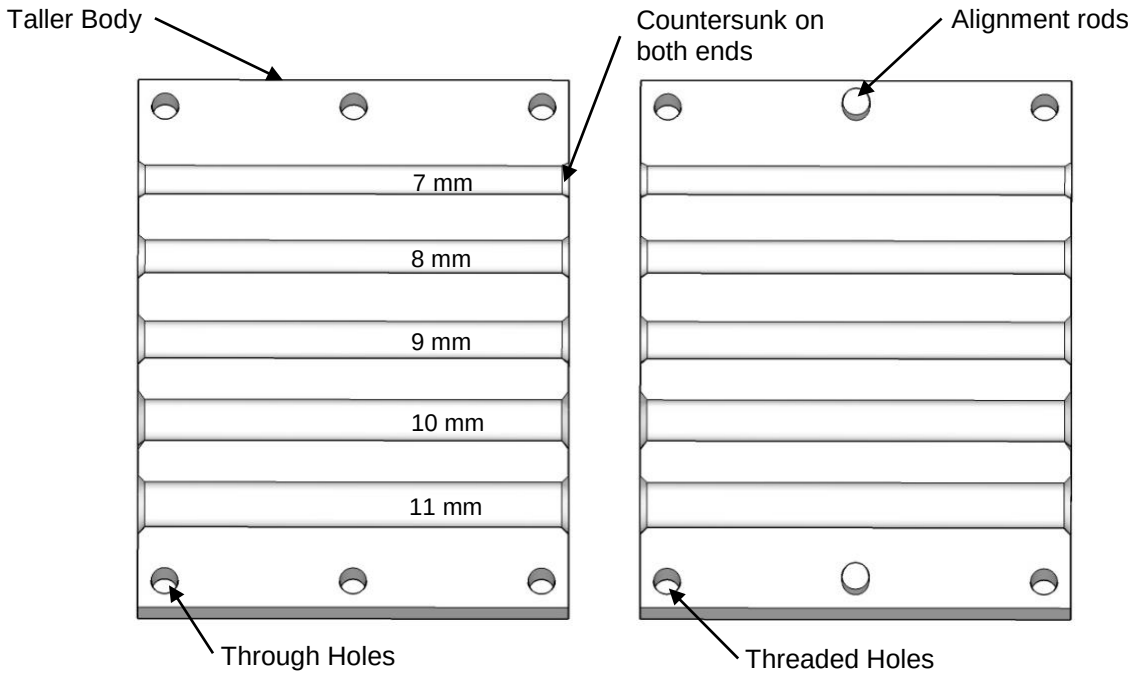

Figure 14: Graphic diagram of the Production Mold with the halves open.

O-rings were used to prevent leaks from the bottom and to center the rod inside the mold. Since the hole sizes changed between layers, the exterior O-rings remained one size that fit within all countersinks, and the interior O-rings were adjusted according to bore size. During air extraction, the top of the mold was kept uncovered to allow an open surface for the bubbles to escape. When curing, a custom weight was used to maintain a seal over the mold opening and bottom O-ring against the countersunk surface. A seal was needed during curing to prevent liquid PDMS from leaking.

Samples made with the Production Mold were multilayered. The first layer always started on the 7 mm bore. The subsequent layers were cured on top of the previous layer. There was also no additional change in the protocol for a new layer except for the addition of an O-ring for each step up in bore size. After each layer was cured, the mold interior was cleaned of any PDMS waste. A colored layer sample was made to distinguish and identify each layer. The colors were also an indicator that the layers did not mix into each other during curing and used for identifying individual ratios. Non colored layered samples were also made for testing on the Biaxial Vascular Testing and Culturing Device to ensure that the colored dye did not influence mechanical properties. The samples were removed from the center rod by removing the O-rings on both ends and pushing them though. Figure 15 shows the multilayered samples made using the optimized protocol from Appendix II with the Production Mold. The first image (A) shows a colored sample still attached to the center rod. Image B and C shows a closer view of the multilayered sample after removal from the rod.

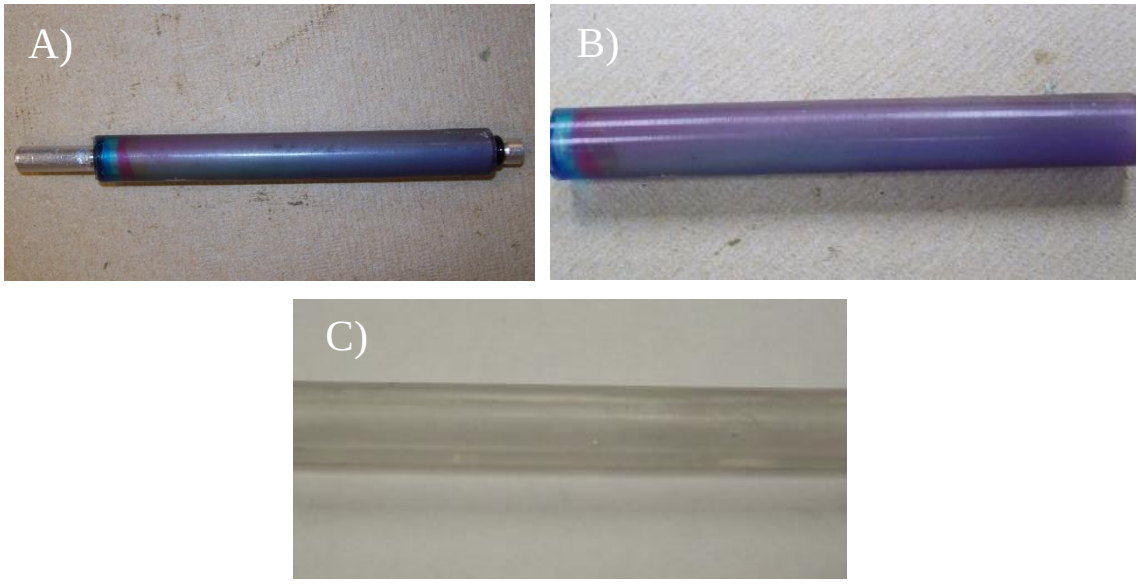

Figure 15: A) Colored sample on new center rod. B) Colored sample after rod removal. C) Clear sample finalized for testing.

2.4.4 Protocol

The optimized protocol was developed after considering the factors and utilizing the latest mold design. The syringe was used as both a mixing and delivery container. The syringe piston was removed and sealed with Parafilm and an 18 gauge probe needle. This assembly was then placed in a holding vessel over a weight scale and used as tare weight for the PDMS components. The curing agent was weighed first and used as tare weight for measuring the polymer base. Both components were mixed and de-aired in the syringe. The Parafilm was removed when the PDMS was ready for dispensing. Figure 16 shows the equipment used for measuring the weight ratios.

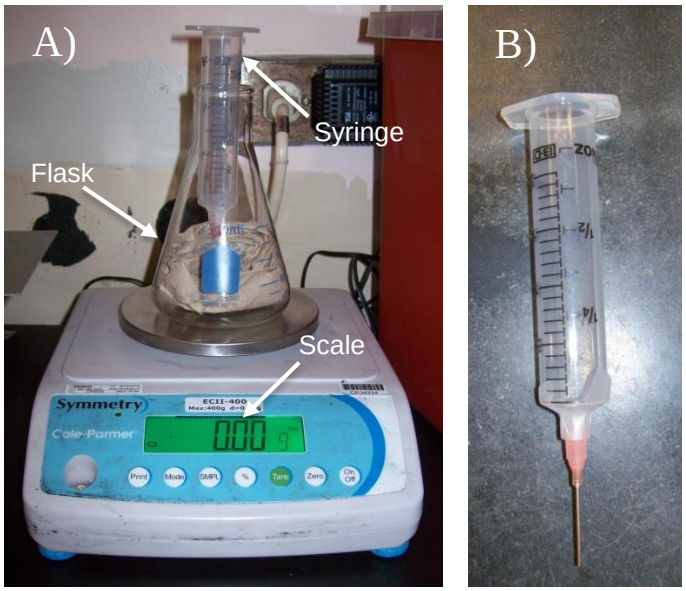

Figure 16: A) Syringe and Erlenmeyer flask holder. This setup used tare weight to measure PDMS ratios and later to dispense the finished mixture. B) Syringe minus piston and sealed with parafilm and dispensing needle.

To improve curing time, the temperature was raised to 100°C and cured for 35-40 minutes. A new syringe was used for each additional layer. As one layer was curing, the next was prepared. The preparation included weighing each PDMS component, mixing, and de-airing. These steps

increased efficiency in the protocol by reducing the total preparation time. The equipment list and the step by step protocol can be found in Appendix I and II.

2.5 Sample Testing Procedure

The samples required custom mounts to fit into the testing device. Each sample was mounted into a male Luer lock fitting at each end and held in place with trimmed rubber hose and a hose clamp. Luer-locks are part of a standardized system of small fittings used in medical and laboratory instruments. The rubber hose served as a buffer to protect the sample from the hose clamp. The fitting used was slightly larger in diameter than the sample so that the tightened fit would help keep the sample in place during stretching. Figure 17 shows the arrangement used for testing.

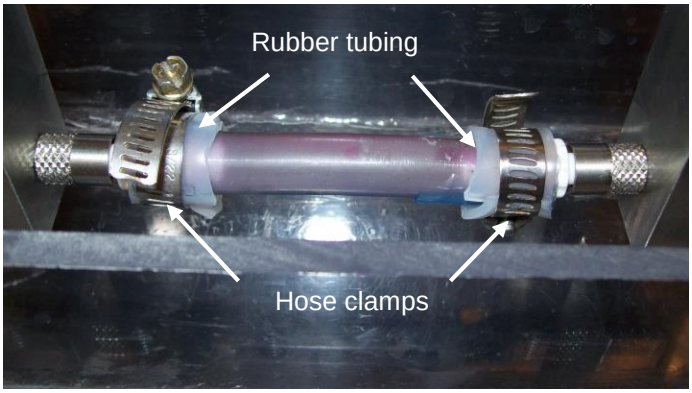

Figure 17: A sample mounted into the Biaxial Vascular Testing and Culturing Device.

All samples were tested with roughly human carotid in vivo conditions by immersing them in temperature controlled saline at 37° C. Transmural pressure was increased by 10 mmHg increments up to 300 mmHg, and then in 50 mmHg up to 500 mmHg. The Biaxial Vascular Testing and Culturing Device setup protocols can be found in Appendix III.

2.5.1 Circumferential Testing

Circumferential testing was performed by varying the transmural pressure at three axial distensions: relaxed, distended 2 mm, and 6 mm. The protocol used for circumferential testing that follows the BVTCD setup can be found in Appendix IV. Figure 3A shows the force direction used in the circumferential testing.

2.5.2 Axial Testing

In axial testing, the stretch ratio is measured from the application of force using stepper motors. The sample was considered to be in a relaxed state after it was mounted and slightly taut along the holder. A 6 mm stretch distance was the maximum length for the samples because the average axial force values reached the transducer limit of 20 Newtons. The maximum limit of the transducer was set to the force value the Biaxial Vascular Testing and Culturing Device used on natural tissue that was stretched beyond 1.5 times its original length. Testing at higher axial force limits would be outside the scope of the project because these values were too high for use on natural arteries. The tests were to compare stretch behavior and not tensile data. Force data was recorded at every 0.5 mm increment. The axial stretch value was determined based on the distance stretched from the relaxed state. The protocol used for axial testing that follows after the BVTCD setup can be found in Appendix V. Figure 3B shows the direction of forces placed on the sample.

2.5.3 Natural Tissue Testing

Natural bovine or pig carotid arteries were tested in the same in vivo conditions as their synthetic counter parts. They were all placed under a 1.5 axial stretch ratio for consistency. This axial stretch placed the samples in a condition where the diameter was uniform throughout the vessel providing a more accurate deformation circumferentially during pressure changes.

Chapter 3

Results

3.0

The samples tested consisted of three 5 layer samples. The first sample was composed of layers that ranged from 10:1 to 5:1. The inner most layer was 10:1, then 8:1 7:1, 6:1 and 5:1 as the last layer. This set of layers is called Layered Sample 1. This sample was dyed with silicon based colors in accordance with Appendix II (10:1=white, 8:1=yellow, 7:1=red, 6:1=green, 5:1=blue). This was to ensure that the layer ratios did not mix into each other between each layer production. The second sample was again composed of Layered Sample 1 ratios with no dye. The third sample was composed of a different ratio set. These ratios ranged from 10:1 to 9:1 at .25 increments, therefore the layers were 10:1, 9.75:1, 9.5:1, 9.25:1, and 9:1. This set of layers was called Layered Sample 2. Since two samples were of the same ratio, all resulting test values for Layered Sample 1 were averaged and used to compare with Layered Sample 2 and other materials. Figure 18 shows a close cross sectional view of how the samples are oriented. The view highlights the individual layers and shows how each layer is distinctively separate from the others. Each layer is labeled with its compositional weight ratio.

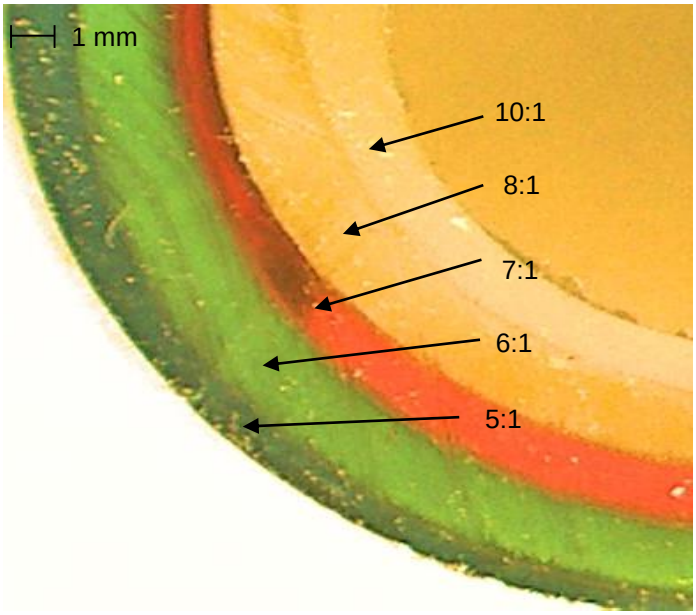

Figure 18: Cross sectional view of a colored Layered Sample 1 sample under a microscope.

3.1 Physical Inspection

From the start of testing the samples were rigid to the touch. This was likely due to the fact that the wall thicknesses of the samples were large in comparison to natural vessels; a limiting factor in the fabrication process. The layers remained in adhesion after manually stretching the samples and no slipping in the axial direction was observed. The average tolerance obtained for the sample outer diameter was ±0.05 mm. The sample thickness was 2.5 mm with an overall length of 80 mm ±1 mm. Individual layers in the clear samples were not distinguishable to the naked eye. When cut axially, the sample layers naturally separated from each other. This was because transitional crosslinks did not form between each layer during the preparation and curing process.

3.2 Circumferential Testing

The outer diameters from circumferential testing are calculated from the images taken for each pressure increment. Image processing was performed to determine specific changes in the outer diameter. Figure 19 shows little change in diameter between the 0 pressure and 300 mmHg images. This was the only visual differences confirmation that the sample was pressurized in the chamber. Figure 19, Figure 20 and Figure 21 show stretching differences can be seen only between the highest and lowest pressure values. Some samples were pressurized up to a maximum 500 mmHg to test the sample stretch in a high pressure condition. Figure 21 shows that the visual stretch between minimum and extreme pressures is significantly visible between the 0 and 500 mmHg pressure values.

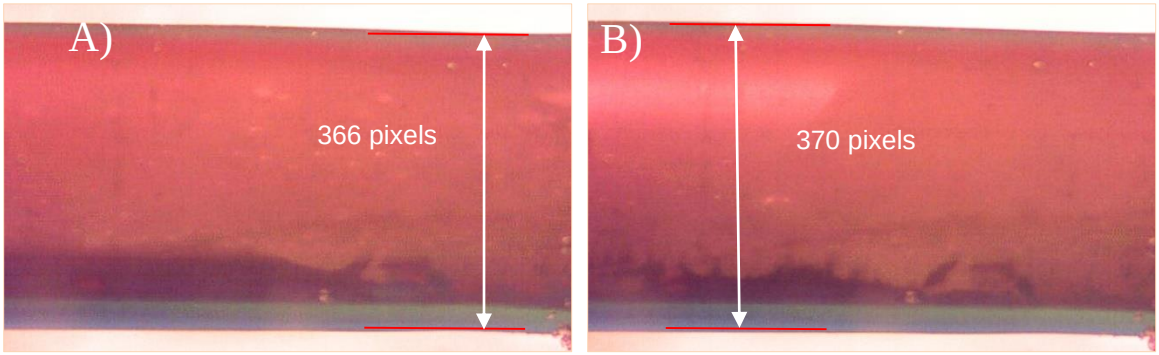

Figure 19: Visual circumferential stretch difference between Layered Sample 1 Colored at Relaxed axial stretch pressurized to A) 0 mmHg and B) 300 mmHg.

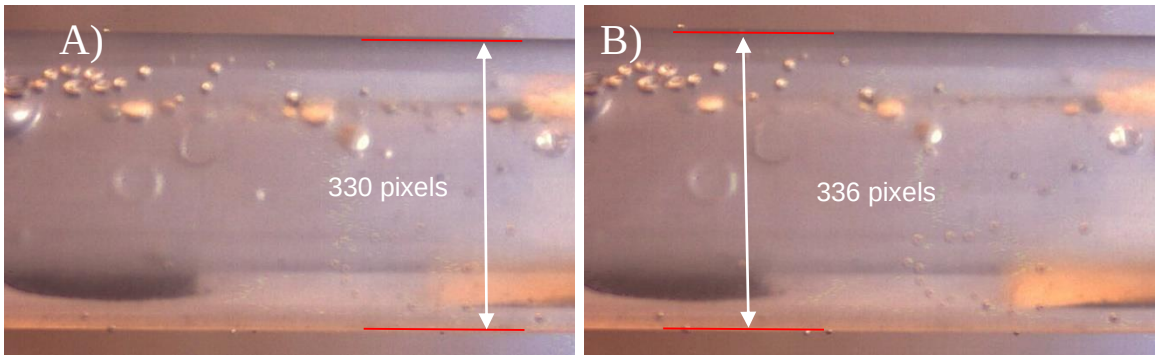

Figure 20: Visual circumferential stretch difference between Layered Sample 2 Clear at 6 mm axial stretch pressurized to A) 0 mmHg and B) 300 mmHg

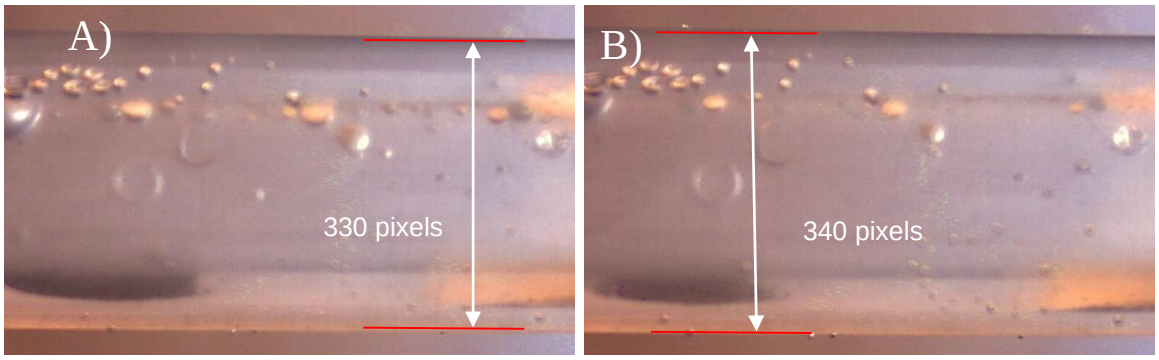

Figure 21: Visual circumferential stretch difference between Layered Sample 2 Clear at 6 mm axial stretch pressurized to A) 0 mmHg and B) 500 mmHg

The data was processed using Microsoft Excel. The stretch ratio was determined using the pixel count of the outer diameter. Outliers in the data were found by graphing the stretch ratio versus the pressure values and removing numbers that far exceeded the grouping. The data was

limited to 300 mmHg pressure range to match the maximum pressure value used in bovine (cow) artery testing. The two sample types were compared in Figure 22 showing the material behavior of pressure vs circumferential stretch. In this graph Layered Sample 2 has a higher stretch ratio than Layered Sample1 for each pressure increment. This is indicated by the amount of pressure required to stretch the sample. The figure shows that Layered Sample 2 required less pressure to stretch at the same rate as Layered Sample 1.

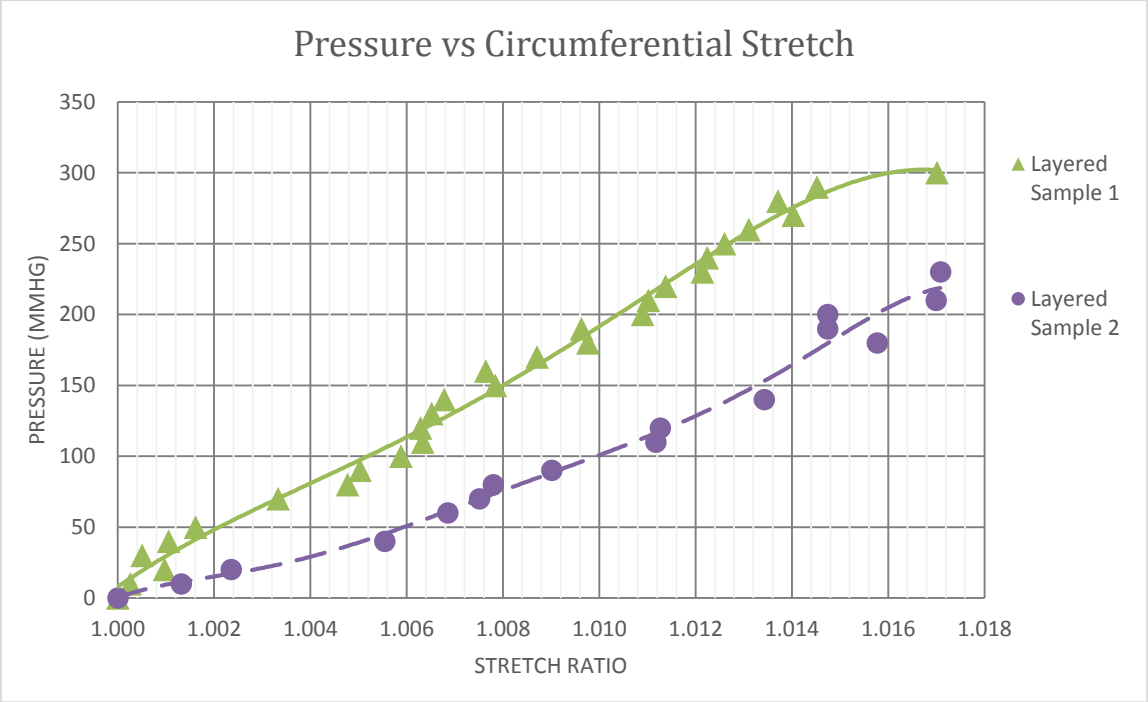

Figure 22: Pressure vs Circumferential Stretch

3.3 Axial Testing

Since axial testing was limited to a 6 mm distension and a force value of 20 N, material behavior can be observed through its force values for every stretch increment. The two samples from Layered Sample 1 were averaged and compared to the Layered Sample 2 sample. Axial stresses are different from circumferential stress in that they are constant throughout the wall and

do not vary along the wall thickness. Figure 23 shows the stretch along the axial direction for each applied force. Layered Sample 2 required less force to stretch axially at the same rate as Layered Sample 1 once the stretch was past a 1.04 ratio.

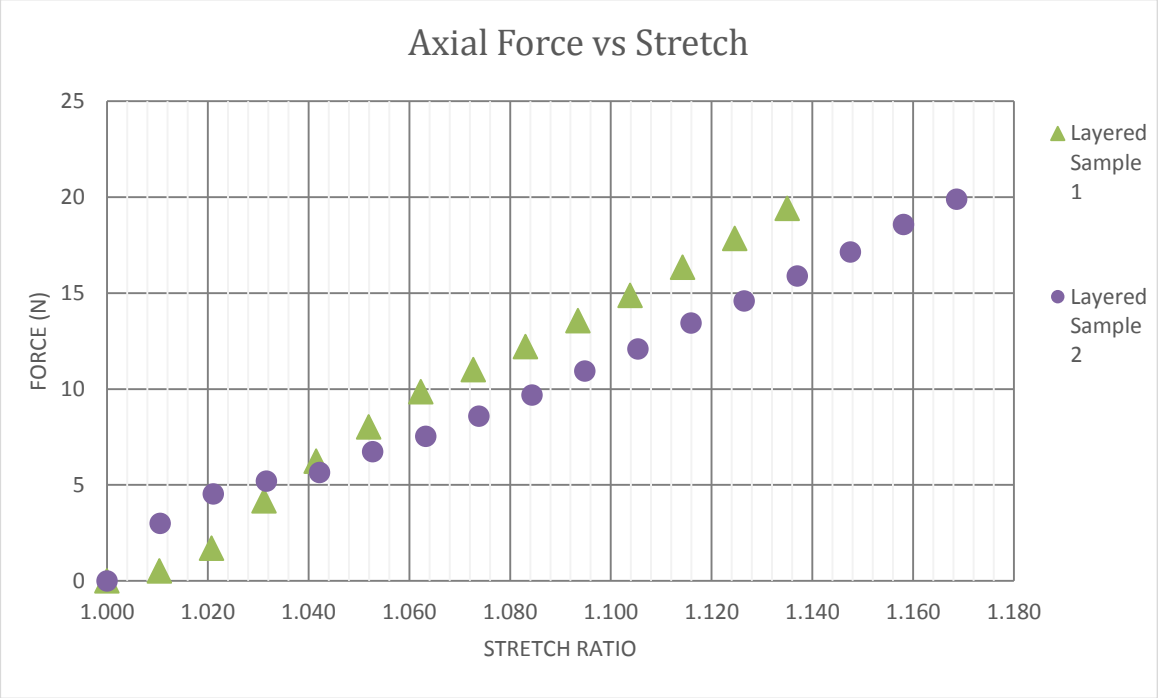

Figure 23: Axial Force vs Stretch

3.4 Data Analysis

In order to determine the mechanical properties of the samples, analysis started with verifying the radius to wall thickness ratio to ensure that the assumption for the equations was accurate. The main assumption for the samples was to consider them as homogenous thick walled cylinders. Another assumption was that the internal radius changed at the same rate as the outer radius. In order to determine the radius of the sample at each pressure change, the value was multiplied by the circumferential stretch ratio.

Stiffness is defined as the amount of measured resistance to deformation and is a property of the structure. In the case of the circumferential data, stiffness is the amount of stretch or displacement for an applied pressure. The circumferential stiffness was considered an important factor in the defining the mechanical properties of the sample because it experienced the most deformation in the BATCD and was not limited to any specific force value like the axial stretch. In the axial data, stiffness is the amount of applied force over a change in length. Since stress is considered constant axially throughout the thickness of the wall, the stiffness along the sample wall can accurately be determined in the circumferential direction. In the axial direction, the layers are parallel to each other and therefore the stiffness, is characterized by a single layer, or in this case, the material. In the circumferential direction, however, the stiffness is defined by the combination of all the layers deforming circumferentially. Figure 24 illustrates the change in cross sectional area for each pressure increment. The straight upward trend of the Layered Sample 1 has a steeper slope compared to Layered Sample 2, indicating a higher stiffness. A stiffness value could be determined by comparing the slopes of the trend lines; a larger slope indicated a stiffer sample. The trend lines are quadratic because they best fit the data. The graph of Layered Sample 1 looks linear compared to Layered Sample 2 because in the comparison between the each other, Layered Sample 2 exhibited the most deformation for each pressure increment. The pressure in the graph is shown in kPa because the unit for stiffness is generally given in the form of a force per unit area. In the case of Figure 24, Layered Sample 1 is more stiff because the change in its cross sectional area is smaller for each pressure change at a rate 20 kPa per mm^2 versus 3 kPa per mm^2 for Layered Sample 2. This was expected because the layer combination for Layered Sample 1 was composed of ratios that were less elastic according to preliminary testing and literature. The ratios that were below 9:1 had a lower modulus of elasticity(Khanafer et al. 2009). So when

combined, the resulting graph showed high stiffness. Layered Sample 2 was composed of ratios between 10:1 and 9:1, where the elastic modulus was the highest(Khanafer et al. 2009). The layer combinations for this sample yielded a higher elastic deformation.

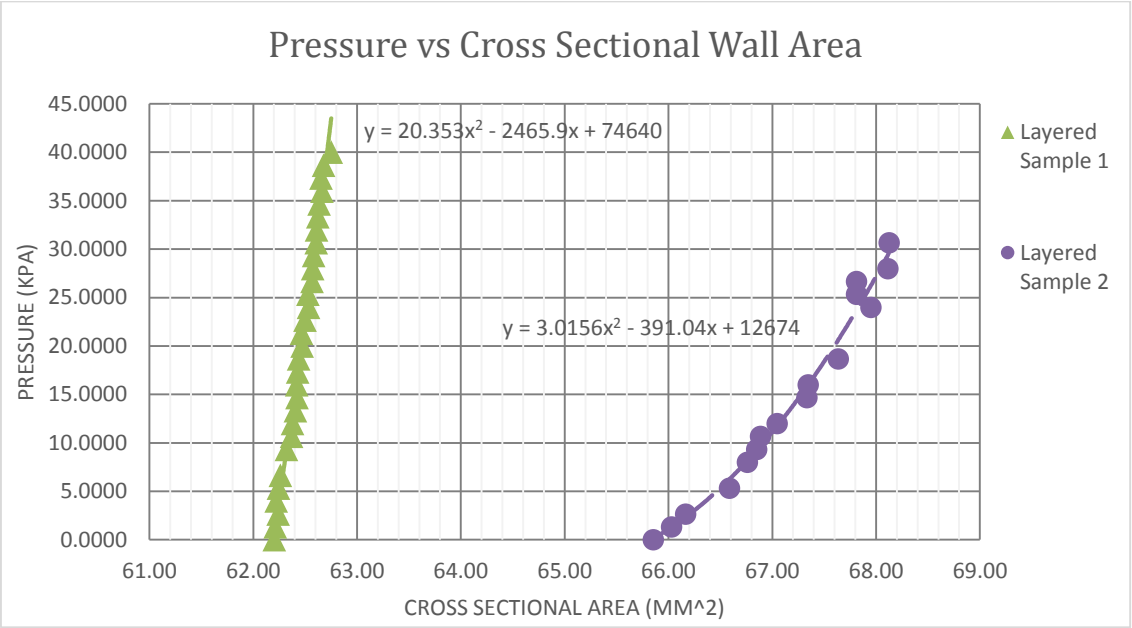

Figure 24: Pressure vs Cross Sectional Wall Area

The rigidity of the samples can be seen in a PDMS comparison to bovine data. In the circumferential stretch graph comparison in Figure 25, the trend shows that the number of layers used in the samples may have been too many. However, in the case of a single layer test, its stretch ratio was significantly higher than the multilayered sample. This single layer sample was tested at a relaxed state and was not axially stretched due to the sample length used. It was half the size of the Layered Sample 1 and 2 samples, and did not have adequate sealing at the attachment sites. The single layer sample was only tested circumferentially. The single layer sample was included to show that the elasticity of PDMS at its manufactured state of 10:1 mixture ratio will require

adjustment in order to reach the stretch levels of natural vessels. Despite the intended biomimicry of the multilayered samples to that of the complex arrangement of cellular layers in natural blood vessels, the results using PDMS were stiff and not what was hypothesized.

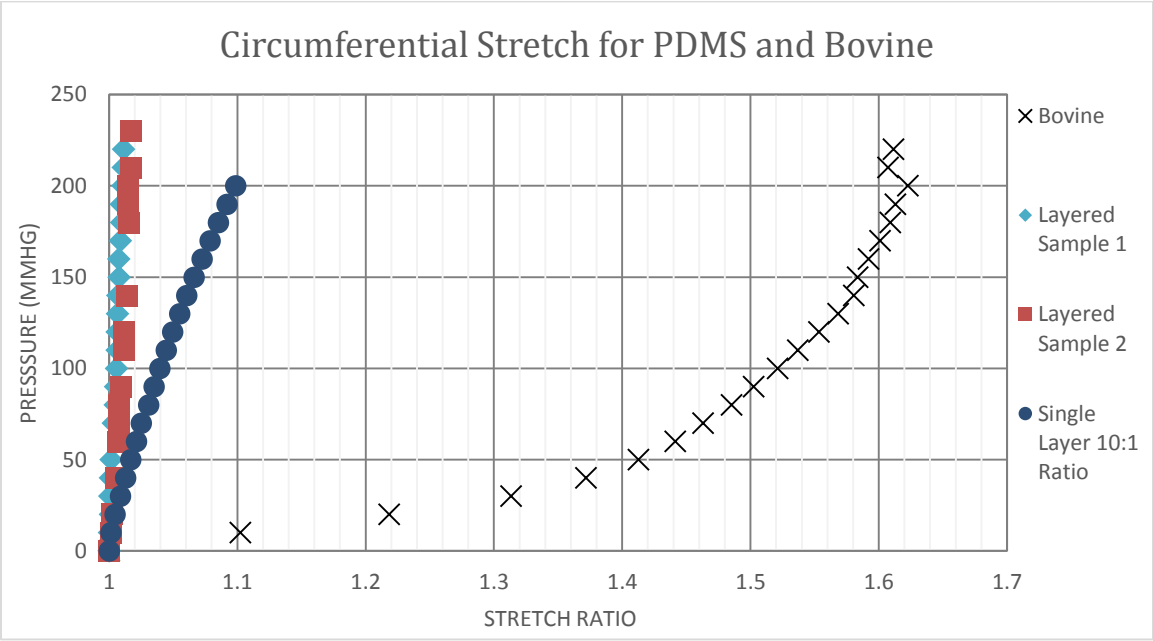

Figure 25: Pressure vs Circumferential Stretch for PDMS and Bovine

Chapter 4

Discussion and Conclusion

4.1 Discussion

The implementation of the optimized protocol with the production mold produced viable samples for biaxial testing. To check for radial heterogeneity, a cross section of the sample was cut and placed in a microscope to view for clarity. The colored sample was chosen because the colors highlighted each layer as shown in Figure 26. This image, taken under a microscope at 10x, shows that the layers did not have air pockets present. This cross section exhibits a clarity that PDMS should have when fully cured. The sample also shows consistency and reliability with the protocol due to the clear separation between each layer.

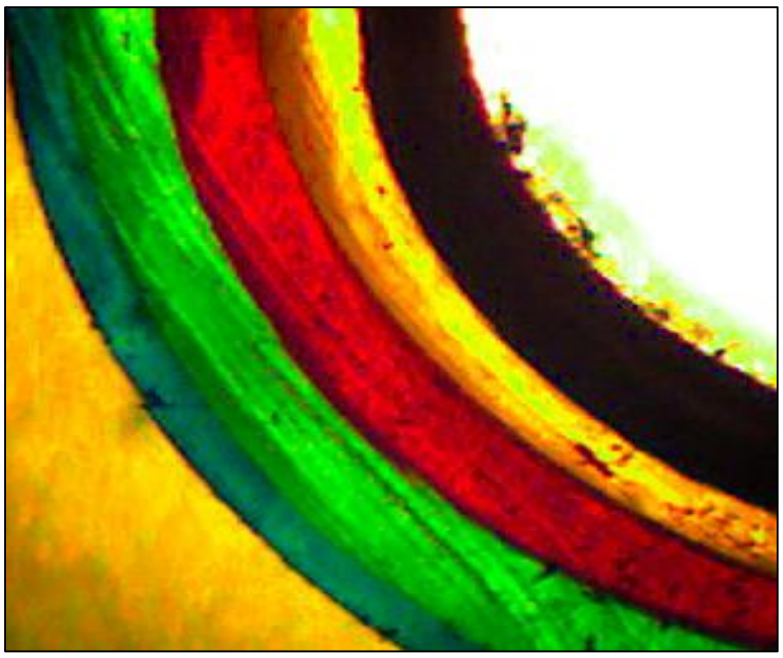

Figure 26: Cross sectional view of a bubble-free colored sample placed under a yellow light.

Clarity shown from a side view in Figure 27 during testing also confirms the optimization of the protocol. White light was shone from the background to highlight the inside diameter and observe changes along the sample wall. The semitransparent walls show that the cylindrical shape

was retained for each layer. The lucidity of each layer's color also show that the base and curing agent were completely mixed and cured into PDMS.

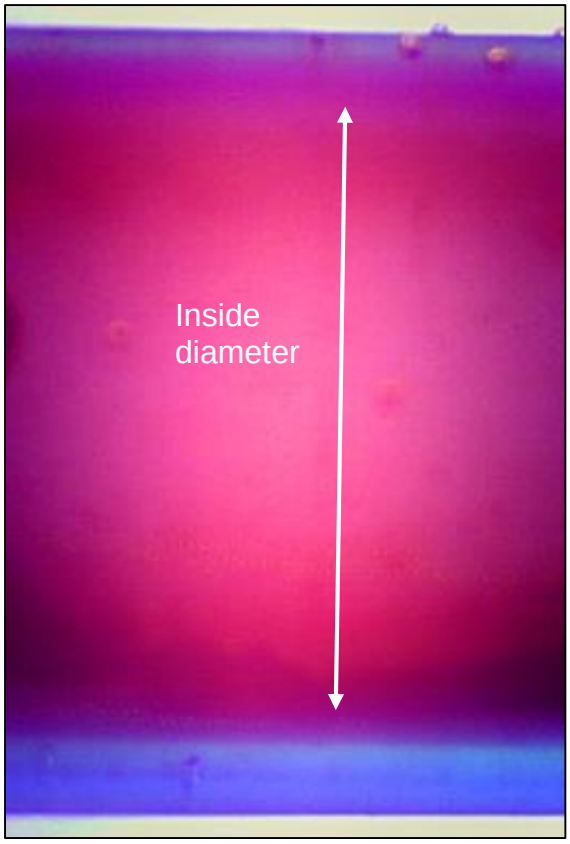

Figure 27: Side view of colored sample.

Some sections that cured in the mold showed gaps in between layers that could be mistaken as air pockets. Polydimethylsiloxane takes the shape of the mold. An example in Figure 28 highlights a small crevice formed in one layer that was inlayed with a polymer of the same composition as the next layer; which formed a blemish that could be mistaken as an air pocket. The formation of this crevice was an indication that the mold interior was not entirely smooth. Figure 29 shows an illustrated cross section depicting how the crevice formed out of the mold cast and the next layer filled in the gap to create the blemish. The depth of the crevice was emphasized to demonstrate the process.

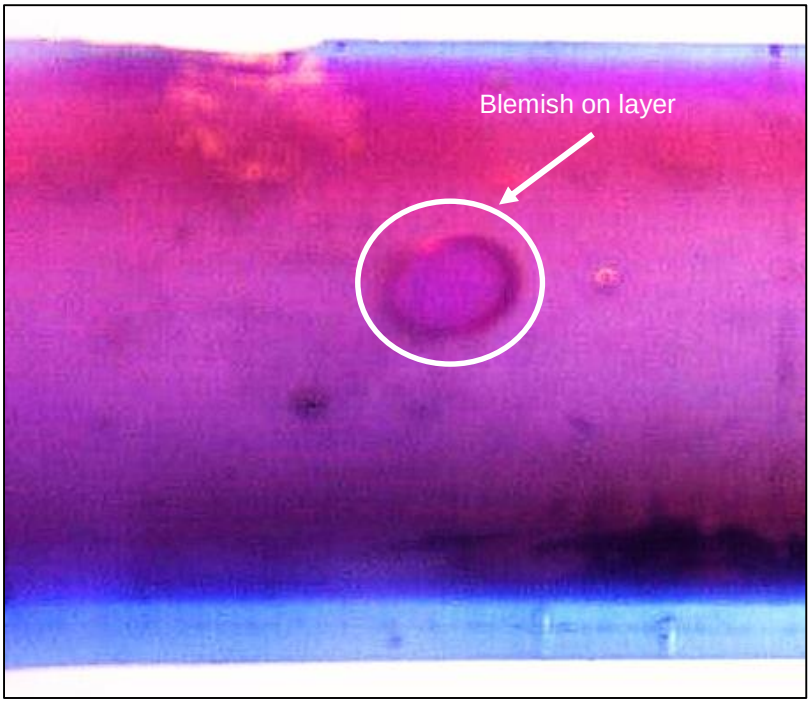

Figure 28: Blemish on a layer. This was a crater formed from one layer that was filled in by the next.

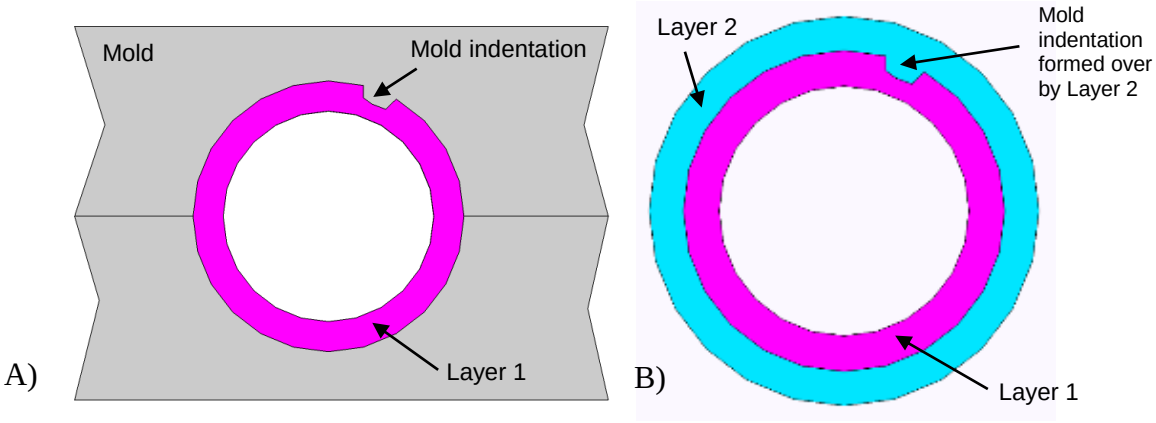

Figure 29: (A) Mold blemish formation starting from the mold face when making Layer 1 (B) and the indentation filled in when forming Layer 2.

Forming a clear and clean uniform sample was greatly emphasized throughout the project, which was why significant efforts were made to reduce and remove air bubbles throughout the sample production. PDMS should cure with a semitransparent clarity. Figure 30 shows the differences between the amounts of air that can be trapped in a sample as evidenced by the number

of air bubbles present. The samples in Figure 30 are all the same ratio (10:1) with a 6 mm inner diameter and 0.5 mm wall thickness. Sample 1 was placed in a sonic bath for air bubble removal while the others used the vacuum desiccator. Sample 2 retained air pockets because it was placed under vacuum for a short amount of time. Sample 3 retains a clean consistency around the edges and was properly de-aired. The clarity and quality of Sample 3 was the requirement for all 5 layers.

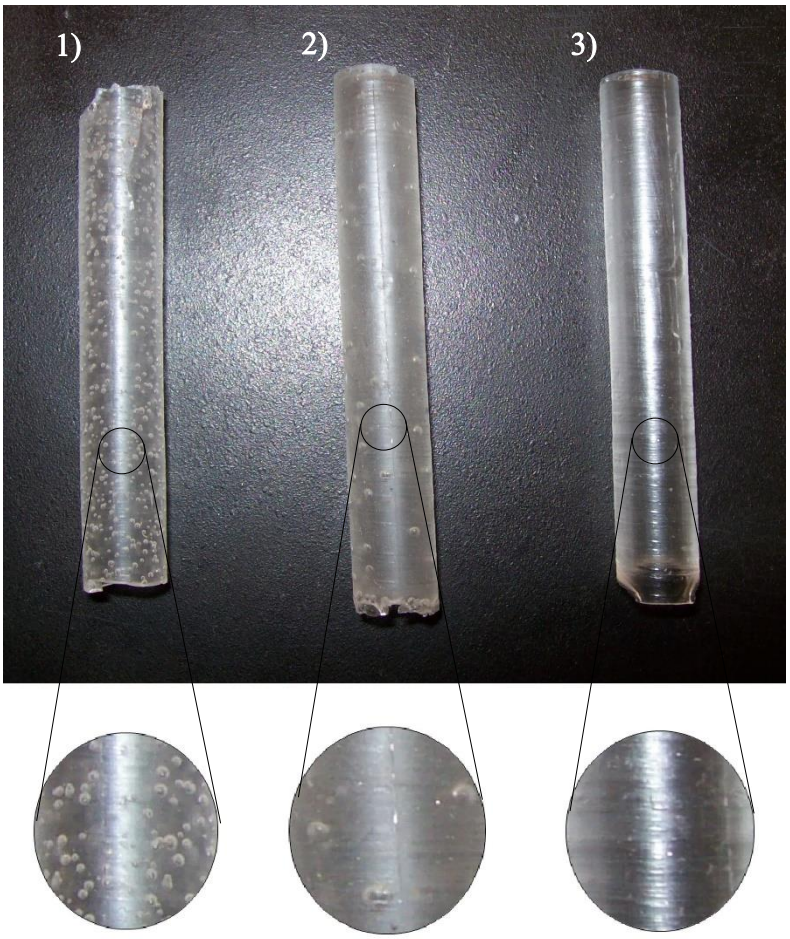

Figure 30: Sample differences between amounts of air pockets as shown in Samples 1-3 where Sample 1 has the most air pockets and Sample 3 does not.

Uniformity within the samples is important, especially between layers. This will create consistent results and improved data. Not all samples had even, uniform layers. The outer layer was the least uniform of all and was tough to create because the ends were not completely centered on the countersink and the angle of tilt from the top caused the wall to be thinner on one side.

The comparison between the mechanical properties of PDMS samples and natural tissue were significantly different. This was due to the 5 layers used in the samples. As more layers were added the composite stiffness in the sample increased. This was shown in the circumferential and axial tests. The circumferential tests revealed that although the sample was capable of sustaining higher pressures, it lacked the proper amount of flexibility a synthetic artery should have. Its high stiffness factor hindered its effectiveness to potentially sustain blood flow.

If each unique layer in the sample, such as the 8:1 ratio, 9:1 ratio, etc, was tested under in vivo conditions, the mechanical behavior of those layers should theoretically be similar to the information obtained from the lab and Khanafer's data; though shifting from 2D to 3D cylindrical tests are not straightforward quantitatively. Samples for each layer should have been made to produce a base stretch definition for individual cylindrical PDMS samples at different ratios, i.e. testing a model with 10:1 ratio, another with 8:1 ratio, etc.

The combination of the different ratios into a single sample created an amalgamation that had its own mechanical property because each ratio layer would mechanically react differently to the applied pressure. The reason for this orientation was to avoid the need to recreate residual stresses in arteries. Residual stresses are stresses that remain within a solid material after all external loads are removed. When an artery stretches due to high pressure, the residual stresses counteract the deformation by contracting the vessel wall (Jay D. Humphrey and Delange 2004). This ensures a minimal stress gradient across the vessel wall promoting uniform expansion. This further prevents vessels from bursting and also helps bring the blood pressure to a level that allows blood flow to circulate. This represents the underlying motivation of the current work.

4.2 Improvements and Future Work

Improvements from this project should include a more precisely machined mold and the use of fewer, and thinner, layers for sample testing. Representation of various layers within natural tissue should focus on the primary layers of a blood vessel, such as the intima (inner most layer), media (the middle section), and adventitia (the outermost layer). A form of material processing was performed in the lab as a separate project that, if successful, was to create porous layers and potentially help improve elasticity. The method was to use salt leaching to create perforations in PDMS in order for fluids to go through (Kannan et al. 2005). Salt leaching embeds salt particles in the cured polymer and later dissolved by placing the sample in water. This process was supposed to create a porous layer and also possibly affect interior dimensions. Further advancement in that experiment would potentially lessen the stiffness in the samples and increase axial and circumferential stretching. An implementation of salt leaching would help bring the PDMS samples closer to mechanomimetic conditions.

Another component that would have helped create improved uniformity along the sample, was the use of an oven. This equipment would have produced an even distribution of heat along the mold body and may also decrease the curing time between layers compared to using a heat plate. Therefore, the production samples with this curing source would potentially have retained quality with less time.

4.3 Conclusion

Natural tissue is a highly complex composite material and difficult to mimic mechanically. This project showed that heterogeneously layered properties of vascular tissue were imitated using Polydimethylsiloxane. Despite the measured mechanical differences, which after all, stemmed from the desire to use "off-the-shelf" materials, multi-layered blood vessel structures were produced with radial heterogeneity. This was the main focus of the project. The methodology can now be applied to more suitable materials for accurate biomimicry.

The process learned here can be applied to other types of materials used for tissue engineering applications. Since the focus of the project was to establish a process for creating synthetic blood vessels with PDMS, the protocols can be applied to other research experiments that use the polymer.

References

Arribas, Silvia M, Aleksander Hinek, and M Carmen González. 2006. “Elastic Fibres and Vascular Structure in Hypertension.” *Pharmacology & Therapeutics* 111 (3) (September): 771–91. doi:10.1016/j.pharmthera.2005.12.003. http://www.ncbi.nlm.nih.gov/pubmed/16488477.

Berdichevsky, Yevgeny, Julia Khandurina, András Guttman, and Y.-H. Lo. 2004. “UV/ozone Modification of Poly(dimethylsiloxane) Microfluidic Channels.” *Sensors and Actuators B: Chemical* 97 (2-3) (February): 402–408. doi:10.1016/j.snb.2003.09.022. http://linkinghub.elsevier.com/retrieve/pii/S0925400503007482.

Borenstein, Jeffrey T, Eli J Weinberg, Brian K Orrick, Cathryn Sundback, Mohammad R Kaazempur-Mofrad, and Joseph P Vacanti. 2007. “Microfabrication of Three-Dimensional Engineered Scaffolds.” *Tissue Engineering* 13 (8) (August): 1837–44. doi:10.1089/ten.2006.0156. http://www.ncbi.nlm.nih.gov/pubmed/17590149.

Borschel, Gregory H, Yen-Chih Huang, Sarah Calve, Ellen M Arruda, Jennifer B Lynch, Douglas E Dow, William M Kuzon, Robert G Dennis, and David L Brown. 2013. “Tissue Engineering of Recellularized Small-Diameter Vascular Grafts.” *Tissue Engineering* 11 (5-6): 778–86. doi:10.1089/ten.2005.11.778. http://www.researchgate.net/publication/7746550_Tissue_engineering_of_recellularized_small-diameter_vascular_grafts?ev=pub_cit.

Buckley, Conor T, Stephen D Thorpe, Fergal J O’Brien, Anthony J Robinson, and Daniel J Kelly. 2009. “The Effect of Concentration, Thermal History and Cell Seeding Density on the Initial Mechanical Properties of Agarose Hydrogels.” *Journal of the Mechanical Behavior of Biomedical Materials* 2 (5) (October): 512–21. doi:10.1016/j.jmbbm.2008.12.007. http://www.ncbi.nlm.nih.gov/pubmed/19627858.

Campbell, G R, and J H Campbell. 2007. “Development of Tissue Engineered Vascular Grafts.” *Current Pharmaceutical Biotechnology* 8 (1) (February): 43–50. http://www.ncbi.nlm.nih.gov/pubmed/17311552.

Chan-Park, Mary B, Jin Ye Shen, Ye Cao, Yun Xiong, Yunxiao Liu, Shahrzad Rayatpisheh, Gavin Chun-Wei Kang, and Howard P Greisler. 2009. “Biomimetic Control of Vascular Smooth Muscle Cell Morphology and Phenotype for Functional Tissue-Engineered Small-Diameter Blood Vessels.” *Journal of Biomedical Materials Research. Part A* 88 (4) (March 15): 1104–21. doi:10.1002/jbm.a.32318. http://www.ncbi.nlm.nih.gov/pubmed/19097157.

Chen, Rui, and John a. Hunt. 2007. “Biomimetic Materials Processing for Tissue-Engineering Processes.” *Journal of Materials Chemistry* 17 (38): 3974. doi:10.1039/b706765h. http://xlink.rsc.org/?DOI=b706765h.

Chen, Yi-chao, and John F. Eberth. 2012. “Constitutive Function, Residual Stress, and State of Uniform Stress in Arteries.” *Journal of the Mechanics and Physics of Solids* 60 (6) (June):

1145–1157. doi:10.1016/j.jmps.2012.02.005. http://linkinghub.elsevier.com/retrieve/pii/S0022509612000361.

Cretich, Marina, Valentina Sedini, Francesco Damin, Gabriele Di Carlo, Claudio Oldani, and Marcella Chiari. 2008. "Functionalization of Poly(dimethylsiloxane) by Chemisorption of Copolymers: DNA Microarrays for Pathogen Detection." *Sensors and Actuators B: Chemical* 132 (1) (May): 258–264. doi:10.1016/j.snb.2008.01.033. http://linkinghub.elsevier.com/retrieve/pii/S0925400508000737.

Enescu, Daniela, Viorica Hamciuc, Lucia Pricop, Thierry Hamaide, Valeria Harabagiu, and Bogdan C. Simionescu. 2008. "Polydimethylsiloxane-Modified Chitosan I. Synthesis and Structural Characterisation of Graft and Crosslinked Copolymers." *Journal of Polymer Research* 16 (1) (June 24): 73–80. doi:10.1007/s10965-008-9204-4. http://www.springerlink.com/index/10.1007/s10965-008-9204-4.

Garra, J., T. Long, J. Currie, T. Schneider, R. White, and M. Paranjape. 2002. "Dry Etching of Polydimethylsiloxane for Microfluidic Systems." *Journal of Vacuum Science & Technology A: Vacuum, Surfaces, and Films* 20 (3): 975. doi:10.1116/1.1460896. http://link.aip.org/link/JVTAD6/v20/i3/p975/s1&Agg=doi.

Grigoriev, G, Z Hess, T Ksander, J Reid, and A Rini. 2011. "Replication of Surface Structures with Polydimethylsiloxane (PDMS Soft Lithography)": 1–6.

Gundiah, Namrata, Mark B Ratcliffe, and Lisa A Pruitt. 2007. "Determination of Strain Energy Function for Arterial Elastin: Experiments Using Histology and Mechanical Tests." *Journal of Biomechanics* 40 (3) (January): 586–94. doi:10.1016/j.jbiomech.2006.02.004. http://www.ncbi.nlm.nih.gov/pubmed/16643925.

Gupta, Siddhi, Satish Sinha, and Arvind Sinha. 2010. "Composition Dependent Mechanical Response of Transparent Poly(vinyl Alcohol) Hydrogels." *Colloids and Surfaces. B, Biointerfaces* 78 (1) (June 15): 115–9. doi:10.1016/j.colsurfb.2010.02.021. http://www.ncbi.nlm.nih.gov/pubmed/20236809.

Hum, Phillip W. 2006. "Exploration of Large Scale Manufacturing of Polydimethylsiloxane (PDMS) Microfluidic Devices."

Humphrey, J D, J F Eberth, W W Dye, and R L Gleason. 2009. "Fundamental Role of Axial Stress in Compensatory Adaptations by Arteries." *Journal of Biomechanics* 42 (1) (January 5): 1–8. doi:10.1016/j.jbiomech.2008.11.011. http://www.pubmedcentral.nih.gov/articlerender.fcgi?artid=2742206&tool=pmcentrez&rendertype=abstract.

Humphrey, Jay D., and Sherry L. Delange. 2004. *An Introduction to Biomechanics: Solids and Fluids, Analysis and Design*. New York: Springer-Verlag.

Jagur-grodzinski, Joseph. 2006. “Polymers for Tissue Engineering , Medical Devices , and Regenerative Medicine . Concise General Review of Recent Studies” (June): 395–418. doi:10.1002/pat.

Kannan, Ruben Y, Henryk J Salacinski, Kevin Sales, Peter Butler, and Alexander M Seifalian. 2005. “The Roles of Tissue Engineering and Vascularisation in the Development of Micro-Vascular Networks: A Review.” *Biomaterials* 26 (14) (May): 1857–75. doi:10.1016/j.biomaterials.2004.07.006. http://www.ncbi.nlm.nih.gov/pubmed/15576160.

Khanafer, Khalil, Ambroise Duprey, Marty Schlicht, and Ramon Berguer. 2009. “Effects of Strain Rate, Mixing Ratio, and Stress-Strain Definition on the Mechanical Behavior of the Polydimethylsiloxane (PDMS) Material as Related to Its Biological Applications.” *Biomedical Microdevices* 11 (2) (April): 503–8. doi:10.1007/s10544-008-9256-6. http://www.ncbi.nlm.nih.gov/pubmed/19058011.

Kim, Tae Kyung, Jeong Koo Kim, and Ok Chan Jeong. 2011. “Measurement of Nonlinear Mechanical Properties of PDMS Elastomer.” *Microelectronic Engineering* 88 (8) (August): 1982–1985. doi:10.1016/j.mee.2010.12.108. http://linkinghub.elsevier.com/retrieve/pii/S0167931710005964.

Klenkler, B J, M Griffith, C Becerril, J a West-Mays, and H Sheardown. 2005. “EGF-Grafted PDMS Surfaces in Artificial Cornea Applications.” *Biomaterials* 26 (35) (December): 7286–96. doi:10.1016/j.biomaterials.2005.05.045. http://www.ncbi.nlm.nih.gov/pubmed/16019066.

Kotz, Kenneth T, and Sunitha Nagrath. 2004. “Lab Module 1: PDMS Fabrication”: 1–4.

Kuo, Alex C M. 1999. “Poly (Dimethylsiloxane)”: 411–435.

Kurkuri, Mahaveer D., Fares Al-Ejeh, Jun Yan Shi, Dennis Palms, Clive Prestidge, Hans J. Griesser, Michael P. Brown, and Benjamin Thierry. 2011. “Plasma Functionalized PDMS Microfluidic Chips: Towards Point-of-Care Capture of Circulating Tumor Cells.” *Journal of Materials Chemistry* 21 (24): 8841. doi:10.1039/c1jm10317b. http://xlink.rsc.org/?DOI=c1jm10317b.

Leclerc, E., Y. Sakai, and T. Fujii. 2013. “A Multi-Layer PDMS Microfluidic Device for Tissue Engineering Applications.” In *The Sixteenth Annual International Conference on Micro Electro Mechanical Systems, 2003. MEMS-03 Kyoto. IEEE*, 415–418. IEEE. doi:10.1109/MEMSYS.2003.1189774. http://ieeexplore.ieee.org/xpl/articleDetails.jsp?reload=true&arnumber=1189774&contentType=Conference+Publications.

Lee, Jessamine Ng, Xingyu Jiang, Declan Ryan, and George M Whitesides. 2004. “Compatibility of Mammalian Cells on Surfaces of Poly(dimethylsiloxane).” *Langmuir : The ACS Journal of Surfaces and Colloids* 20 (26) (December 21): 11684–91. doi:10.1021/la048562+. http://www.ncbi.nlm.nih.gov/pubmed/15595798.

Lillie, M a, and J M Gosline. 2007. “Limits to the Durability of Arterial Elastic Tissue.” *Biomaterials* 28 (11) (April): 2021–31. doi:10.1016/j.biomaterials.2007.01.016. http://www.ncbi.nlm.nih.gov/pubmed/17240445.

Linder, V, E Verpoorte, W Thormann, N F de Rooij, and H Sigrist. 2001. “Surface Biopassivation of Replicated Poly(dimethylsiloxane) Microfluidic Channels and Application to Heterogeneous Immunoreaction with on-Chip Fluorescence Detection.” *Analytical Chemistry* 73 (17) (September 1): 4181–9. http://www.ncbi.nlm.nih.gov/pubmed/11569807.

Lopez, Analette I, Amit Kumar, Megan R Planas, Yan Li, Thuy V Nguyen, and Chengzhi Cai. 2011. “Biofunctionalization of Silicone Polymers Using Poly(amidoamine) Dendrimers and a Mannose Derivative for Prolonged Interference against Pathogen Colonization.” *Biomaterials* 32 (19) (July): 4336–46. doi:10.1016/j.biomaterials.2011.02.056. http://www.pubmedcentral.nih.gov/articlerender.fcgi?artid=3085595&tool=pmcentrez&rendertype=abstract.

Mata, Alvaro, Aaron J Fleischman, and Shuvo Roy. 2005. “Characterization of Polydimethylsiloxane (PDMS) Properties for Biomedical Micro/nanosystems.” *Biomedical Microdevices* 7 (4) (December): 281–93. doi:10.1007/s10544-005-6070-2. http://www.ncbi.nlm.nih.gov/pubmed/16404506.

Myung, David, Wongun Koh, Jungmin Ko, Yin Hu, Michael Carrasco, Jaan Noolandi, Christopher N. Ta, and Curtis W. Frank. 2007. “Biomimetic Strain Hardening in Interpenetrating Polymer Network Hydrogels.” *Polymer* 48 (18) (August): 5376–5387. doi:10.1016/j.polymer.2007.06.070. http://linkinghub.elsevier.com/retrieve/pii/S0032386107006842.

Nerem, R M, and D Seliktar. 2001. “Vascular Tissue Engineering.” *Annual Review of Biomedical Engineering* 3 (January): 225–43. doi:10.1146/annurev.bioeng.3.1.225. http://www.ncbi.nlm.nih.gov/pubmed/11447063.

Peterson, L. H., R. E. Jensen, and J. Parnell. 1960. “Mechanical Properties of Arteries in Vivo.” *Circulation Research* 8 (3) (May 1): 622–639. doi:10.1161/01.RES.8.3.622. http://circres.ahajournals.org/cgi/doi/10.1161/01.RES.8.3.622.

Quake, S R, and A Scherer. 2000. “From Micro- to Nanofabrication with Soft Materials.” *Science (New York, N.Y.)* 290 (5496) (November 24): 1536–40. http://www.ncbi.nlm.nih.gov/pubmed/11090344.

Roger, Véronique L, Alan S Go, Donald M Lloyd-Jones, Emelia J Benjamin, Jarett D Berry, William B Borden, Dawn M Bravata, et al. 2012. “Executive Summary: Heart Disease and Stroke Statistics--2012 Update: A Report from the American Heart Association.” *Circulation* 125 (1) (January 3): 188–97. doi:10.1161/CIR.0b013e3182456d46. http://www.ncbi.nlm.nih.gov/pubmed/22215894.

Sarkar, Sandip, Thomas Schmitz-Rixen, George Hamilton, and Alexander M Seifalian. 2007. "Achieving the Ideal Properties for Vascular Bypass Grafts Using a Tissue Engineered Approach: A Review." *Medical & Biological Engineering & Computing* 45 (4) (April): 327–36. doi:10.1007/s11517-007-0176-z. http://www.ncbi.nlm.nih.gov/pubmed/17340153.

Serini, Volker. 2002. "Polycarbonates." *Ullmann's Encyclopedia of Industrial Chemistry*. doi:10.1002/14356007.a21_207.

Songmene, V, R Khettabi, I Zaghbani, J Kouam, and A Djebara. 1983. "Machining and Machinability of Aluminum Alloys."

Subhash, G., Q. Liu, D. F. Moore, P. G. Ifju, and M. a. Haile. 2010. "Concentration Dependence of Tensile Behavior in Agarose Gel Using Digital Image Correlation." *Experimental Mechanics* 51 (2) (April 14): 255–262. doi:10.1007/s11340-010-9354-2. http://www.springerlink.com/index/10.1007/s11340-010-9354-2.

Wang, Xueya, Marc P Wolf, Rahel Bänziger Keel, Roman Lehner, and Patrick R Hunziker. 2012. "Polydimethylsiloxane Embedded Mouse Aorta Ex Vivo Perfusion Model: Proof-of-Concept Study Focusing on Atherosclerosis." *Journal of Biomedical Optics* 17 (7) (July): 076006. doi:10.1117/1.JBO.17.7.076006. http://www.ncbi.nlm.nih.gov/pubmed/22894489.

Xue, Lian, and Howard P Greisler. 2003. "Biomaterials in the Development and Future of Vascular Grafts." *Journal of Vascular Surgery* 37 (2) (February): 472–80. doi:10.1067/mva.2003.88. http://www.ncbi.nlm.nih.gov/pubmed/12563226.

Yang, Jian, Antonio R Webb, Samuel J Pickerill, Gretchen Hageman, and Guillermo a Ameer. 2006. "Synthesis and Evaluation of Poly(diol Citrate) Biodegradable Elastomers." *Biomaterials* 27 (9) (March): 1889–98. doi:10.1016/j.biomaterials.2005.05.106. http://www.ncbi.nlm.nih.gov/pubmed/16290904.

Young, Hugh D. 1992. *University Physics*. 7th ed. Addison Wesley.

Yow, K-H, J Ingram, S A Korossis, E Ingham, and S Homer-Vanniasinkam. 2006. "Tissue Engineering of Vascular Conduits." *The British Journal of Surgery* 93 (6) (June): 652–61. doi:10.1002/bjs.5343. http://www.ncbi.nlm.nih.gov/pubmed/16703652.

Zhang, Wen Jie, Wei Liu, Lei Cui, and Yilin Cao. 2007. "Tissue Engineering of Blood Vessel." *Journal of Cellular and Molecular Medicine* 11 (5): 945–57. doi:10.1111/j.1582-4934.2007.00099.x. http://www.ncbi.nlm.nih.gov/pubmed/17979876.

Appendix I

Equipment used in the mixture preparation.

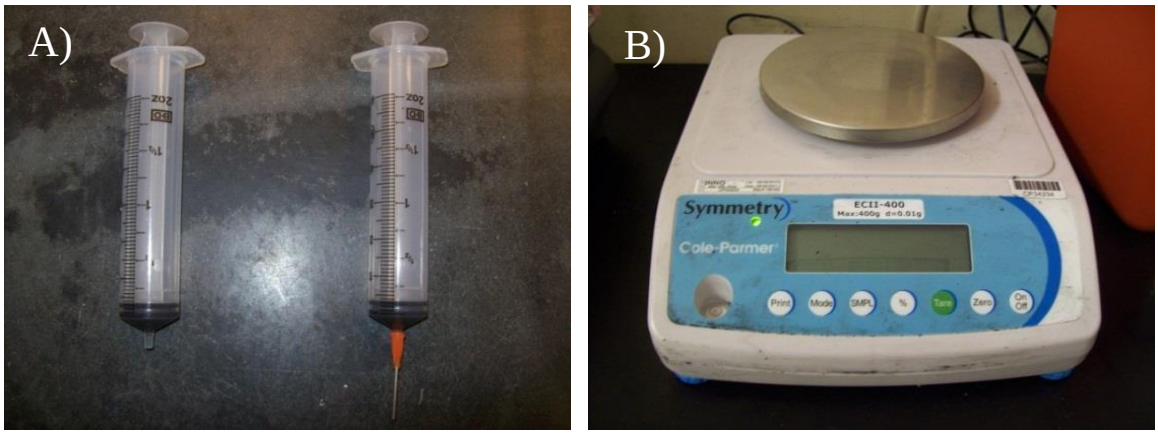

Figure 31: a) 30 mL syringes used to extract base polymer and curing agent B) Cole Parmer Weighing Scale

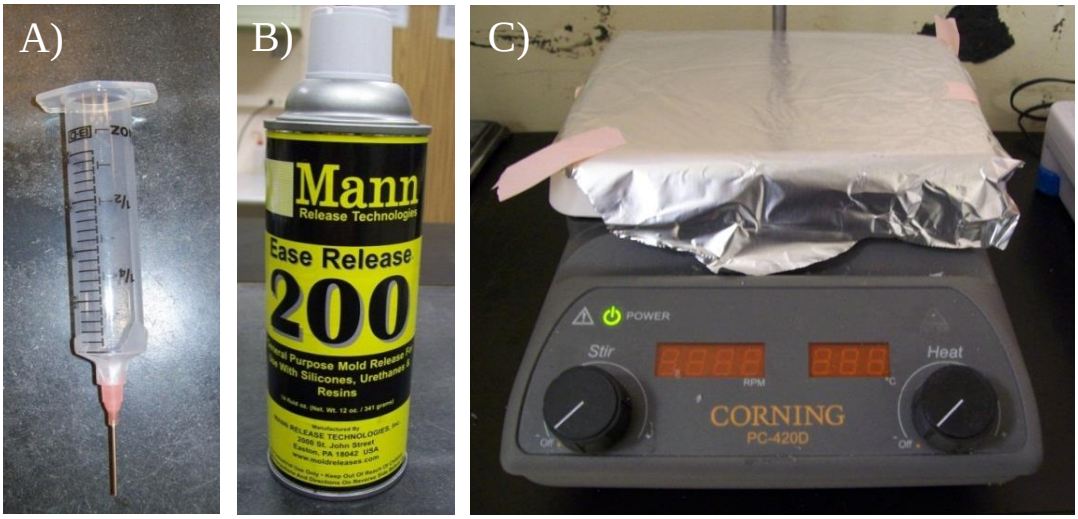

Figure 32:A) 20 mL syringe without plunger B) Ease Release 200 C) Corning PC-4200 hotplate

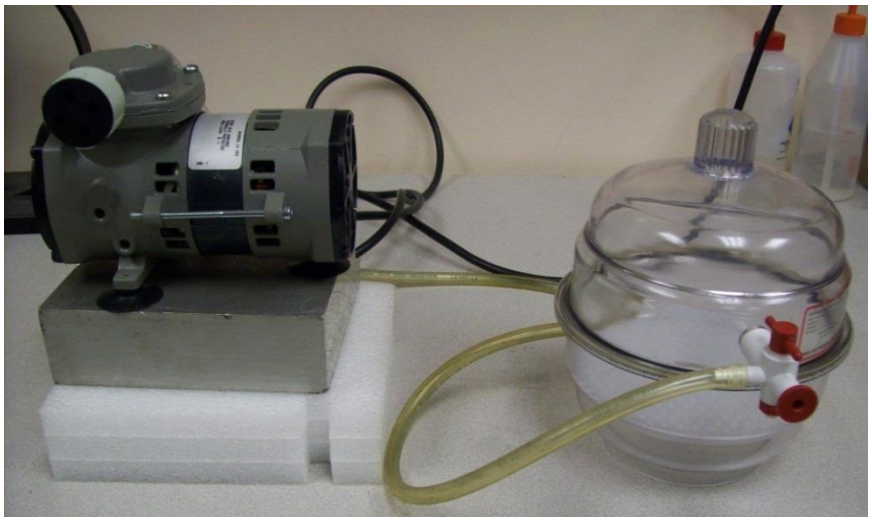

Figure 33: Vacuum Pump and Vacuum Desiccator

Appendix II

PDMS Sample Blood Vessel Preparation Protocol Using a Mold

1. Equipment Preparation
    1.1. Preheat hotplate to 100°C
    1.2. Spray mold and center rod with Ease Release 200. Ease Release takes 5 minutes to set before use.
    1.3. Remove plunger from PDMS syringe container
    1.4. Seal end of syringe body with Parafilm and hold in place with 18 gauge dispensing needle
    1.5. Place container body into a holder over weight scale
    1.6. Tare the scale to zero
    1.7. Open 2 large 30 mL syringes. Attach one 18 gauge dispensing needle on one syringe tip. This will be used to extract the polymer Curing Agent. The other large syringe will be for the polymer base.
    1.8. Determine what ratio to make and calculate amount needed based on weight.
2. PDMS Mixing
    2.1. Extract the curing agent first. Remove an approximate amount based on specific ratio.
    2.2. Slowly dispense curing agent in syringe until ratio weight desired is reached. Repeat 2.1 if more material is needed. Place extra curing agent in waste bin.
    2.3. Record value and tare the scale to zero.
    2.4. Extract polymer base using second large syringe. Remove amount as needed per ratio.

2.5. Slowly dispense polymer base into syringe container until ratio weight is reached. Repeat 2.4 if more material is needed. Place extra polymer base in waste bin.

2.6. Place a small drop of silicon dye in accordance with ratio type using a glass stirring rod. Use a small drop and use sparingly. The following table was used to distinguish color with ratio type.

Table 2: Ratio and Corresponding Dye Color

Ratio	Color
10:1	
8:1	
7:1	
6:1	
5:1	

NOTE: This step was only used to identify the layers and not required during production. This was included to indicate the color scheme that represented the

varied stiffness from the different ratios. The colors were placed from light to dark, where the lightest was the most pliable.

2.7. Stir the mixture thoroughly to combine the polymer base and curing agent and the dye (if used).

3. PDMS Air Removal

3.1. Place the syringe container in vacuum desiccator and close tightly.

3.2. Make sure vacuum pump is connected to vacuum desiccator valve and turn on.

3.3. Leave vacuum pump on for 15 minutes to de-air entire container.

4. Dispensing Preparation

4.1. After air bubbles settle, place the syringe plunger that was removed from Step 1.3 into the bottom of the syringe body to prevent the PDMS from spilling when tilted.

4.2. Tilt syringe tip upwards and remove parafilm.

4.3. Press plunger into syringe body until flush with PDMS mixture.

4.4. The syringe should have a bubble free liquid PDMS mixture with an 18 gauge needle dispenser tip and plunger.

4.5. The mixture is ready for dispensing into a mold.

5. Mold Dispensing

5.1. Align mold halves so the opposite ends line up with each other

5.2. Slowly inject liquid PDMS into one side filling about half of the canal. Cover the entire length of the mold interior.

5.3. Place center rod in the middle with the end O-rings attached on both ends. Make sure the O-rings are flush with the countersink surfaces and the smaller interior O-rings for the bottom end are in place.

5.4. Slowly inject liquid PDMS into the other half and filling it the same amount as the previous half.

5.5. Quickly join both halves along the guide rods and tighten all mold screws. Make sure to tighten the screws firmly to reduce interior leaks.

5.6. Wipe excess PDMS

6. Mold air removal

6.1. Place mold standing up inside the vacuum desiccator on top of a paper towel.

6.2. Slide top O-ring upward along the center rod to leave space for the air bubbles to escape.

6.3. Close the vacuum desiccator and ensure that the chamber is fully sealed around the mold.

6.4. Turn on vacuum pump and vacuum air for 20 minutes.

NOTE: Vacuum times may vary according to sample wall thickness. Thin walls require more time for bubbles to rise to the surface.

7. Curing

7.1. After air removal, slide the top O-ring back into the countersink.

7.2. Place mold on hotplate and secure sides to prevent the mold from tipping over.

7.3. Place weight on top of rod and top O-ring.

7.4. Cure for 35 minutes at 100°C.

7.5. After the allotted time, remove the mold from the hotplate and leave out to cool.

8. Sample Removal

8.1. Unscrew the holding screws on the mold and slowly separate the halves.

8.2. Hold the center rod against the right half while completely removing the left half.

8.3. The sample should stay on the mold half and not be removed.

8.4. Using a scalpel or sharp knife, cut along the mold edge by the cured PDMS to remove waste. The cuts should only be along the metal surface edge so the sample can keep its round shape.

8.5. Remove O-rings from the ends of the center rod.

8.6. If creating another layer, keep the cured PDMS on the center rod. Clean the mold by wiping it down and making sure that all cured PDMS waste is removed. Spray the next bore size up with Ease Release and repeat the process from step one. The only exception is to NOT spray the center rod since the first layer is already one it. Spraying the center rod with Ease Release while there is a cured PDMS layer currently on it will ruin the layer and will require a new one. Ensure that the interior O-ring is the correct size for the bore on the next layer.

8.7. If all layers have been created, remove all O-rings and slowly push the sample out of the center rod.

8.8. Clean the sample by soaking it in Deionized water.

Appendix III

Biaxial Vascular Testing and Culturing Device Setup Protocol

i. Turn on device and all conjoining components.

ii. Connect all components of the BVTCD (DAQ, force and pressure transducer, pressure controller, adventitial and transmural peristaltic pumps, water heater, stepper motors, and camera).

iii. Run BVTCD LabVIEW file (Compiled .vi).

iv. Run camera software.

v. Adjust camera optics to required zoom.

vi. Zero both stepper motors to full retraction position.

vii. Zero the force transducer.

viii. Pump saline solution through adventitial and transmural flow lines.

ix. Add saline solution to the bath.

x. Circulate adventitial flow to allow saline in bath to equilibrate to 37°C.

xi. Mount the sample to descending arms using male luer lock fittings.

    a. Use dispensing needles or barbed fittings with female luer lock end as inserts for the sample.

    b. Hold sample down using hose clamps. Use a piece of tubing as a protective sheath between the hose clamp and sample to prevent tearing.

xii. Attach descending arms to mount. Move mount position using stepper motors to appropriate length.

xiii. Ensure that the sample is taut (not compressed or stretched) after mounting.

xiv. Circulate transmural flow lines and remove all air pockets. Make sure enough saline remains within the compliance chamber.

xv. Zero pressure transducer.

xvi. Condition sample by axially stretching (moving stepper motors cyclically to appropriate axial stretches) and circumferential stretching (gradually increasing and decreasing the transmural pressure using the pressure controller).

Appendix IV

The following testing protocols follow immediately after the BVTCD Setup Protocols.

Circumferential Testing Protocol

i. Return sample to relaxed axial stretch state and ~0 mmHg of transmural pressure.

ii. Save an image of the sample using the camera software.

iii. Increase pressure by 10 mmHg.

iv. Save an image of the sample.

v. Repeat steps ii and iii until appropriate max transmural pressure is reached (300 or 500 mmHg).

vi. Repeat steps i-iv with varying axial stretch states (2 and 6mm stretch)

Appendix V

The following testing protocols follow immediately after the BVTCD Setup Protocols.

Axial Testing Protocol

i. Return the sample to relaxed axial stretch state.

ii. Increase transmural pressure to 100 mmHg.

iii. Record force transducer measurement.

iv. Increase axial stretch by appropriate amount (0.5mm).

v. Repeat steps iii and iv until appropriate max axial stretch/force is reached.

NOTE: Do not exceed 20 Newton's of force measured by force transducer.